PROMOTioN
PROGRESS ON MESHED HVDC OFFSHORE TRANSMISSION NETWORKS

D10.2: Evaluation of the Interaction of Circuit Breaker sub-components with the Test-Circuit during the Interruption Process

PROMOTioN – Progress on Meshed HVDC Offshore Transmission Networks
Mail info@promotion-offshore.net
Web www.promotion-offshore.net

This result is part of a project that has received funding form the European Union's Horizon 2020 research and innovation programme under grant agreement No 691714.

CONTACT

DOCUMENT INFO SHEET

Document Name:	Report Describing the Specification, Design and Implementation of Experimental DC Circuit Breaker
Responsible partner:	DNV GL
Work Package:	WP10
Work Package leader:	Rene Smeets
Task:	10.2
Task lead:	Nadew Belda

DISTRIBUTION LIST

APPROVALS

	Name	Company
Validated by:	Ali Bidadfar	DTU
Validated by:	Dr. Klaus Würflinger	SIEMENS
Task leader:	Nadew Belda	DNV GL
WP Leader:	Rene Smeets	DNV GL

DOCUMENT HISTORY

Version	Date	Main modification	Author
1.0	13-11-2018	Draft table of contents	Nadew Belda
2.0	07-12-2018	Total content of the deliverable	Nadew Belda, Rene Smeets

WP Number	WP Title	Person months	Start month	End month
WP10	Circuit Breaker Performance Demonstration		25	48

Deliverable Number	Deliverable Title	Type	Dissemination level	Due Date
10.2	Evaluation of the interaction of circuit breaker sub-components with the circuit during the interruption process	Deliverable	Classified information	

LIST OF CONTRIBUTORS

Work Package and deliverable involve a large number of partners and contributors. The names of the partners, who contributed to the present deliverable, are presented in the following table.

PARTNER	NAME
DNV GL	Nadew Belda, Rene Smeets, Cornelis Plet

Content

EXECUTIVE SUMMARY

HVDC circuit breakers interact with their surroundings during the current interruption process. This could be the HVDC grid in the practical operation or the test environment during testing at a test facility. In order to study this interaction, access to internal measurements of sub-component stresses is necessary. Due to confidentiality issues it is difficult to get access to internal measurements of manufacturers' prototype breakers. In addition, the test results with the detailed measurements including test failure conditions are publicly shared within the project consortium. Therefore, an "experimental DC CB" is set-up in KEMA Laboratories by putting commercially available, standard components already in use in the laboratory, combined with a few specially designed systems, together. An active injection DC CB is set-up as most of the components such as current injection circuit (including pre-charged capacitor, and inductor), a fast-making switch (plasma triggered spark gaps) and the main interrupter (i.e. the vacuum circuit breaker) are all readily available in the laboratory. For energy absorption, metal oxide surge arrester (MOSA) stacks needed for this purpose are specified, designed, and realized. Since this is an essential component common to all HVDC circuit breaker technologies, special focus has been given to the design procedure of MOSA, and this procedure is discussed in detail in this document.

It must be noted that the purpose of setting up an experimental DC CB is not to investigate the performance of the overall set-up, rather to study the stresses on individual components by producing the stresses observed in actual DC circuit breakers. The results of this study will serve to provide guidelines on application of the proper stresses in testing.

This project has received funding from the European Union's Horizon 2020 research and innovation programme under grant agreement No 691714.

1. INTRODUCTION

1.1 PURPOSE

HVDC circuit breaker is a system of components put together to achieve DC current interruption function. During operation (current interruption process) these components interact among each other as well as with their surroundings and hence, see different kinds of stresses. For the purpose of studying internal sub-component stresses, access to measurements within the HVDC circuit breaker is required. For investigation of internal sub-component stresses, an experimental type HVDC circuit breaker is set up at the test laboratory of DNV GL, KEMA Laboratories. The main objective being not the overall performance but investigation of the limits of standard components (used in DC circuit breakers) in terms of electrical stresses to which these components are subjected during short-circuit current interruption. The major components investigated are vacuum interrupter and metal oxide surge arresters. The main purpose of this document is to provide information regarding the design of the experimental DC CB, component specification and instrumentation used for this investigation. In addition, the important design steps, for example, design procedures of metal oxide surge arrester for DC CB application and test procedures during the column matching are described in detail. The tolerance assumed during matching and a few oscillograms obtained during the column matching process are provided.

The actual test results of the experimental DC CB are provided in Deliverables 10.3 and 10.4 which shall follow this deliverable.

1.2 MOTIVATION

The motivation is to evaluate interaction between HVDC circuit breaker and its electrical environment during the current interruption process. Thus, the set-up of an experimental type DC CB enables to perform extensive investigation on the relationship between performance limit and the rate-of-rise of fault current, current interruption, fault current commutation, counter voltage generation and energy absorption. The tests are intended to find the limits of DC CB components with respect to critical parameters such as rate of change of current at current zero through the vacuum circuit breaker (VCB), the arc duration and arc energy, and the gap length of VCB. In addition, current sharing and energy handling capability of MOSA, the maximum energy limit of MOSA, etc. are investigated. For this reason, the experimental HVDC CB is set-up with the focus on investigation of subcomponent stresses. This document provides specification and design of the major components of the experimental HVDC CB along with the instrumentation necessary to quantify the stresses.

1.3 DOCUMENT STRUCTURE

The rest of this document is organized as follows. Chapter 2 presents the detail of the main components of the experimental DC CB. Chapter 3 provides discussion of the main electrical and thermal parameters of the experimental DC CB to be investigated. And finally Chapter 4 presents an example case test result of an experimental DC CB.

This project has received funding from the European Union's Horizon 2020 research and innovation programme under grant agreement No 691714.

2. SPECIFICATION OF COMPONENTS OF THE EXPERIMENTAL HVDC CIRCUIT-BREAKER

In order to investigate the performance limits of the individual sub-components, it is necessary to have access to the internal measurements of a test object. Thus, an experimental DC circuit breaker based on active current injection is set-up in a laboratory environment. Although, slightly different configurations can be realized, the electrical diagram of a general set-up is shown in Figure 2-1.

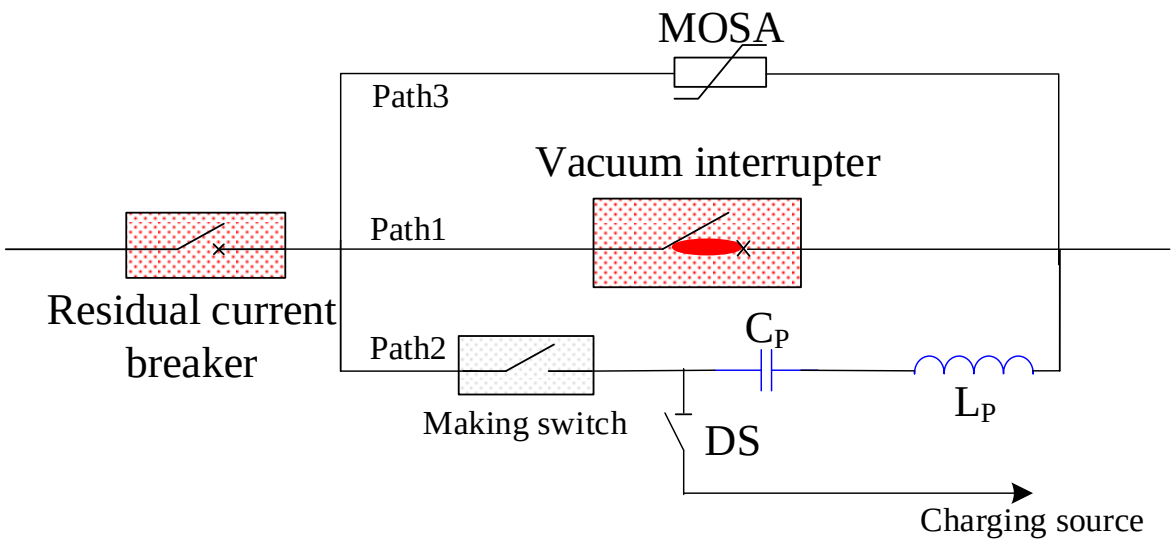

Figure 2-1: Schematic of experimental HVDC Circuit Breaker

The major components of focus are

- The vacuum interrupter or circuit breaker
- The metal oxide surge arrester (MOSA)
- The injection circuit (CP and LP)

With regard to the injection circuit, the focus is to obtain optimal capacitor-inductor (L-C) circuit (frequency, charging voltage and injection current amplitude) that can accommodate both the large current interruptions as well as low current interruptions. This boil down to the range of di/dt that the vacuum interrupter can handle during current interruption [1], [2]. In addition to di/dt at current zero, the impact of other factors such as arcing duration, arc energy, gap length and various contact types are investigated.

2.1. SPECIFICATION OF THE VACUUM CIRCUIT BREAKERS USED AS MAIN INTERRUPTER

Compared to other current interruption media such as gas, air or oil, vacuum as current interruption medium is suitable for DC CB applications. Some of the reasons are,

This project has received funding from the European Union's Horizon 2020 research and innovation programme under grant agreement No 691714.

- Compared to other circuit breakers, a VCB is simple and requires less drive energy needed to operate the contacts. Thus, it can be combined with customized, very fast drive mechanisms for HVDC applications
- A vacuum interrupter can clear much higher di/dt at current zero and can re-gain dielectric strength quicker and hence, can withstand very high du/dt after current zero compared to gas-based media
- Small gap length is enough to obtain dielectric strength

There are some drawbacks of vacuum interrupters

- Prone to re-ignitions and late re-strikes
- Prone to current chopping although this is not a concern for HVDC circuit breaker application

The inner and outer view of typical vacuum interrupters are shown in Figure 2-2 a) and b), respectively, while a typical three-phase vacuum circuit breaker is shown in Figure 2-3. A vacuum circuit breaker includes vacuum interrupter and the drive mechanism. One of the main differences between the VCB for AC CB application and VCB for DC CB application is the operating mechanism. The vacuum circuit breaker used in the HVDC CBs has a very fast operating mechanism/drive, for example based on Thomson Coil actuators, which rapidly opens its contacts upon receiving a trip command from the protection system. Thus, the contacts of the vacuum interrupter separate within a few milliseconds from the moment of trip command. Whereas, the VCBs used in AC applications have slower operating mechanisms that results in delay of up to tens of milliseconds from trip command until the contacts of the vacuum interrupter separate. Typically, it takes up to 30 – 50 milliseconds from the moment of receiving trip command until the contacts of AC VCB separate.

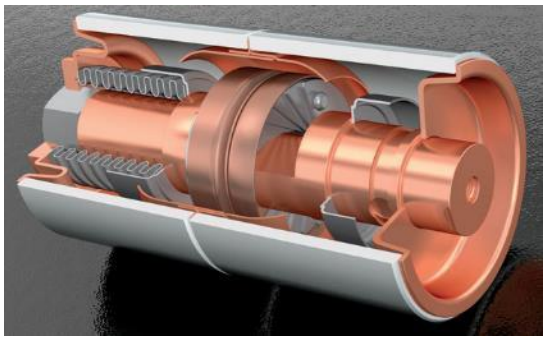

a)

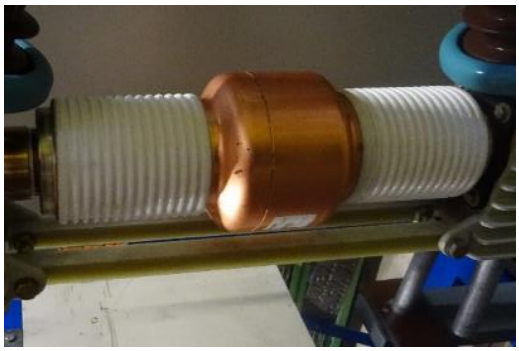

b)

Figure 2-2: a) Inner view of a vacuum interrupter b) Outer view of a vacuum interrupter

This project has received funding from the European Union's Horizon 2020 research and innovation programme under grant agreement No 691714.

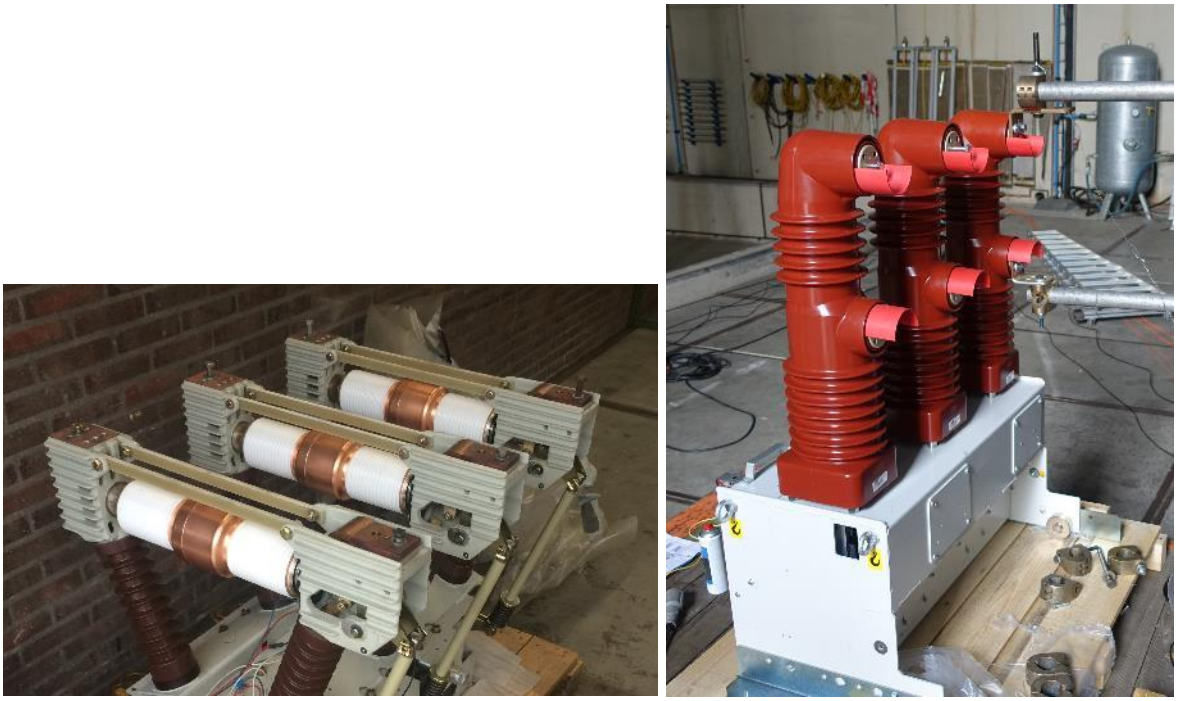

Figure 2-3: Three-phase AC vacuum circuit breakers

In both applications (AC and DC, CB), once the contacts of the vacuum interrupter are separated, an electrical arc is established in the vacuum medium. From this moment onwards, the vacuum medium behaves similar for both AC and DC application. Thus, the main difference between the two applications is, therefore, the time duration from the trip command until contact separation. Although the time from trip command until contact separation is crucial for overall performance of DC CB, it is not considered in this investigation since the drive mechanism is designed for AC current interruption applications. Thus, this study focuses on the behaviour of vacuum interrupter and vacuum medium under different current interruption conditions from contact separation onwards.

The performance of vacuum interrupters at different stages of current interruption process depends on the contact design, contact materials, composition, etc. In order to take the differences in the design of interrupter contacts into account, three standard off-the-shelf vacuum circuit breakers produced by various manufacturers are used.

The specification of the three different vacuum circuit breakers used in the experimental DC CB are shown in Table 1.

Table 1: Specifications of VCBs used in the experimental DC CB

VCB type	Voltage rating (, rms, kV)	Current rating (rms, kA)	Short-circuit current rating (rms, KA)	Opening time (ms)
Type A	38	2.5	31.5	37
Type B	36	2.5	40	46.6
Type C	36	2.0	31.5	37

This project has received funding from the European Union's Horizon 2020 research and innovation programme under grant agreement No 691714.

The vacuum circuit breaker type A used in the experimental DC CB is a special design circuit breaker, optimized for very high electrical endurance (arc furnace breaker). In addition, each of the phase poles can be controlled and operated independently, though this feature is not used in this test campaign.

2.2. SPECIFICATION AND DESIGN OF METAL OXIDE SURGE ARRESTER (MOSA) FOR DC CB APPLICATION

A peculiar feature of HVDC circuit breaker during current interruption process is absorption of magnetic energy stored in the system inductance. Any HVDC circuit breaker technology has a dedicated part to absorb this energy. The energy absorption part of the HVDC circuit breaker constitutes specially designed Metal Oxide Surge Arresters (MOSA). This part is made of metal oxide resistor blocks (also known as varistors) designed and arranged in multiple columns to absorb the system energy without significant deterioration.

A few major differences between the use of surge arresters for over voltage protection (both in AC and DC applications) and for HVDC circuit breaker applications are highlighted in Table 2.

Table 2: Major differences in surge arrester usage for over voltage protection in AC and DC systems and energy absorption HVDC circuit breaker application

Surge arrester for over voltage protection in AC and DC[1] systems	**Surge arresters for HVDC circuit breaker application**
Active all the time /conducts leakage current	Passive during normal operation of the system – become involved only during DC CB operation
Subject to system voltage under normal operation	Does not see system voltage during normal operation
One or a few columns are enough (low energy absorption required)	Large number of parallel columns needed for high energy absorption
Very short duration (<< 1 ms) of energy application	Energy absorption duration in several (<10 ms) range
Limits current following during over voltage	Suppresses fault current from its peak value

In the design of MOSA for HVDC circuit breaker application, there are critical parameters which need to be understood. Before delving into the detail of these parameters, a basic introduction to the differences between various metal oxide varistor blocks are discussed in the proceeding subsection.

2.2.1. CHARACTERIZING METAL OXIDE VARISTOR – IMPACT OF HEIGHT AND DIAMETER ON I-V CHARACTERISTICS

One of the most important parameters of metal oxide varistor that must be known/specified is the I-V characteristics. There are three separate operation regions on the I-V curve as depicted in Figure 2-4; namely,

[1] For thermal energy rating of surge arresters in HVDC applications, the energy value comes from system study. (IEC 60099-9 version 1, 2014)

This project has received funding from the European Union's Horizon 2020 research and innovation programme under grant agreement No 691714.

pre-breakdown, **breakdown,** and **high-current** region. The figure shows I-V characteristics in relation to AC system surge protection application.

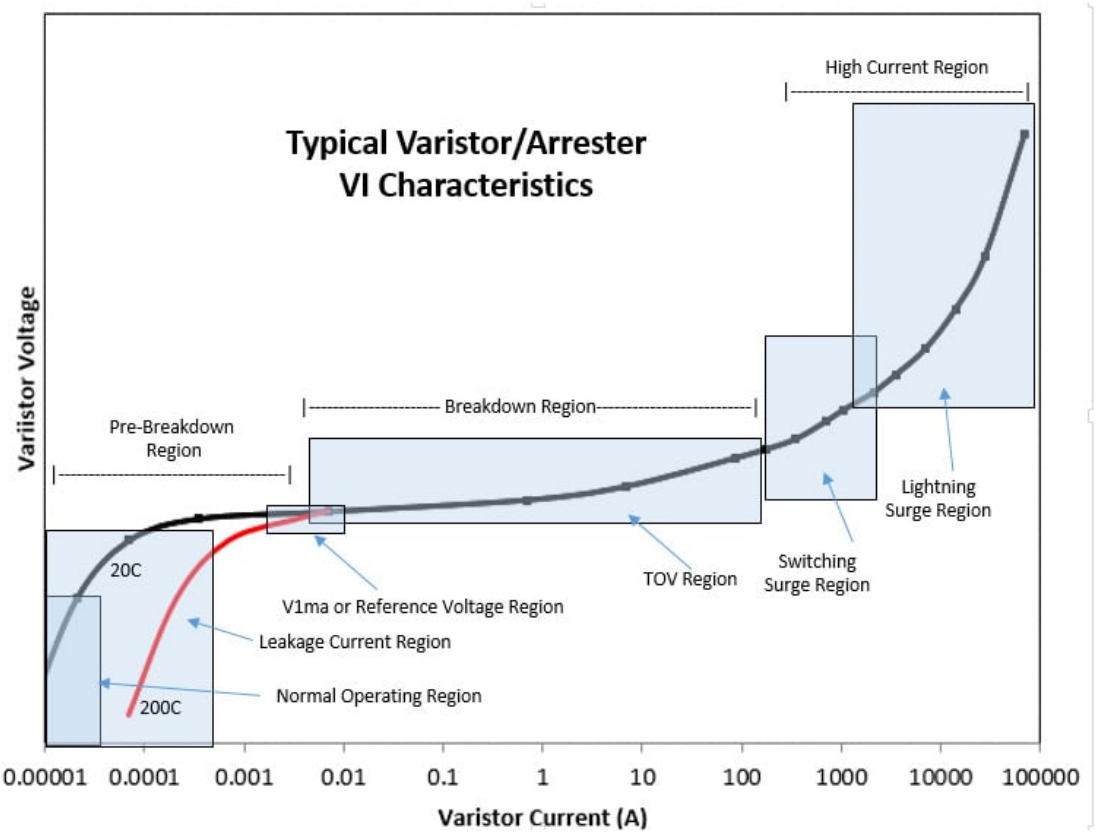

Figure 2-4: Understanding I-V characteristics of varistor blocks (source: [3])

The most interesting region for HVDC circuit breaker application is the breakdown region and lower side of high-current region where a very small change in voltage across the varistor results in significant change in current through the varistor or vice versa. An HVDC circuit breaker designer needs to know the corresponding voltage at a given current or vice versa, in relation to the current interruption rating of the breaker. This relationship is not only depends on electrical parameters, but also physical dimensions of the varistor blocks; namely, diameter, more precisely surface area, and height. In order to understand the impact of diameter and height on the I-V characteristics of varistor blocks, three samples of varistor blocks, shown in Figure 2-5, with different dimensions (diameter and height) are compared by applying 8/20 lightning impulse. The dimensions of the selected samples are shown Table 3.

This project has received funding from the European Union's Horizon 2020 research and innovation programme under grant agreement No 691714.

Sample 1 Sample 2 Sample 3

a) Side view of MO varistors (showing height differences)

b) Top view of various MO – varistors (showing diameter differences)

Figure 2-5: Three different samples of MO varistors having different dimensions selected for demonstrating the I-V characteristics

Table 3: Dimension of the three selected samples

Dimension	Sample 1	Sample 2	Sample 3
Diameter (mm)	69.88	77.92	98.84
Height (mm)	6.34	18.45	9.44

A test set-up with a 8/20 lightning impulse generator is arranged and each of the samples are tested. All these tests were carried out at Darmstadt Technical University, Darmstadt, Germany. Here, the voltage of the impulse source, the voltage across the varistor block, impulse current through the varistor block, current rise time and current falling time are measured. In addition, energy absorbed during each impulse is also computed from the measured current and voltage. After each impulse test the surface temperatures of the varistors are measured using an infrared thermometer. The procedure and the test set-up are shown in Figure 2-6.

This project has received funding from the European Union's Horizon 2020 research and innovation programme under grant agreement No 691714.

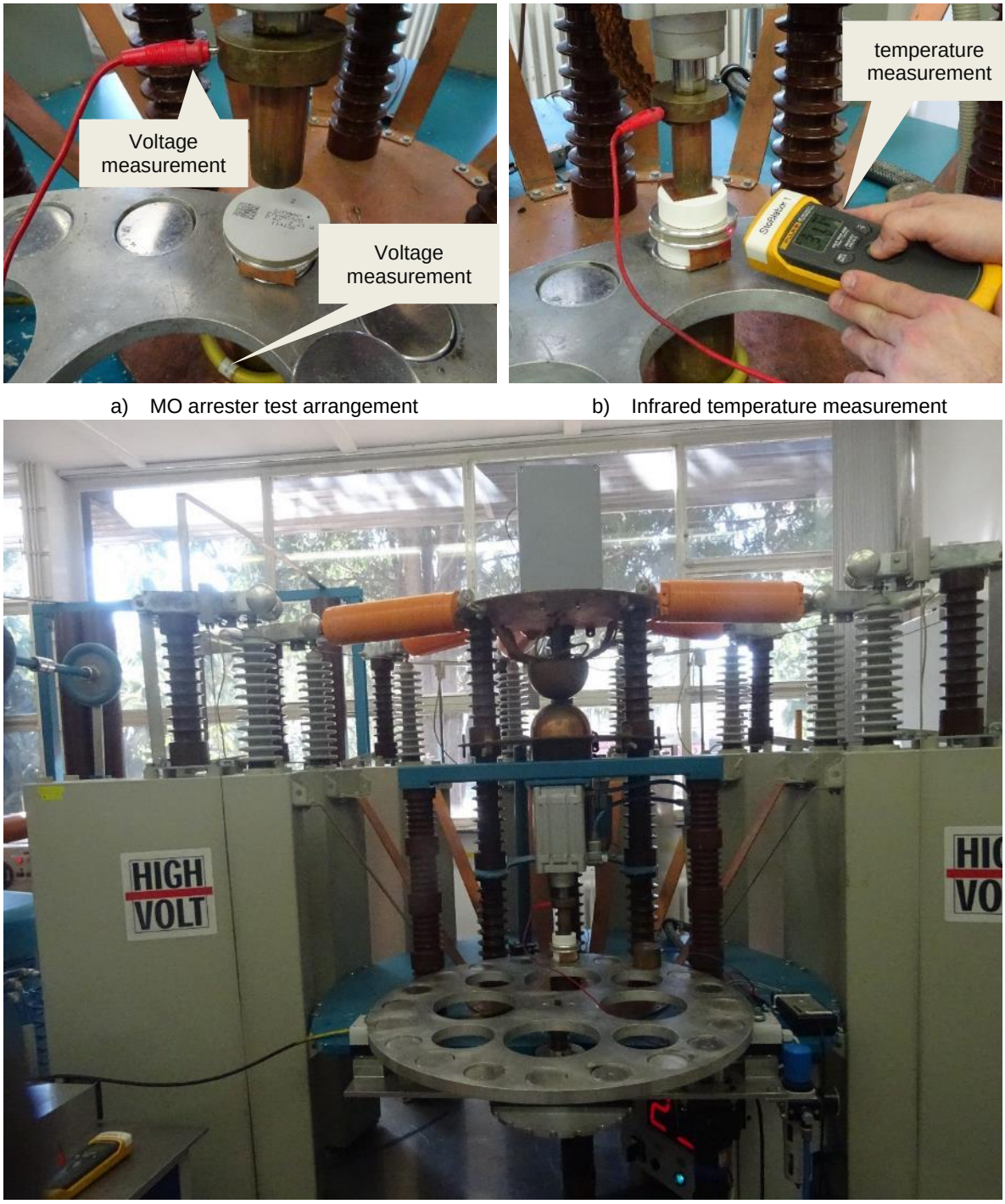

a) MO arrester test arrangement

b) Infrared temperature measurement

c) Test set-up for 8/20 impulse test

Figure 2-6: Test set-up for applying different 8/20 lightning impulses to characterize the I-V characteristic of different varistor blocks

Using the set-up and procedure shown in Figure 2-6 several impulse shots are performed. Figure 2-7 shows the test results of typical impulse current through and voltage across the MO varistor samples. The main aim in these impulse tests is to experimentally highlight the differences in I-V characteristics of the three selected samples by keeping the impulse source parameters (charging voltage and circuit) unchanged. In this case, the impulse source

This project has received funding from the European Union's Horizon 2020 research and innovation programme under grant agreement No 691714.

capacitor is charged to a voltage of 8 kV. It can be observed from Figure 2-7 that the resulting impulse current and voltage of each varistor is different from one another. From Table 3, varistor sample 1 has diameter of 69.88 mm with height 6.34 mm. When an impulse from a capacitor charged to 8 kV is applied, the residual voltage of peak value 2.01 kV appears across the varistor. At this voltage a discharge current with peak value of 5.29 kA flow through this sample. When the same impulse source is applied across varistor sample 2, it produces a residual voltage with peak value 4.68 kV and discharge current of peak value 2.98 kA. Comparing the two varistors (sample 1 and sample 2), sample 1 has about a third of the height of sample 2 and the diameter is lower by about 9 mm. The voltage across the varistor is related to the height of the varistor block while the current through the varistor block depends on the surface area perpendicular to the current flow. Varistor sample 3 has intermediate height among the three samples but the largest diameter of all. Thus, the voltage across sample 3, with same impulse source as for the other two samples, is 2.29 kV (higher than for sample 1 but lower than sample 2) and the current measured through this sample at this residual voltage is 5 kA.

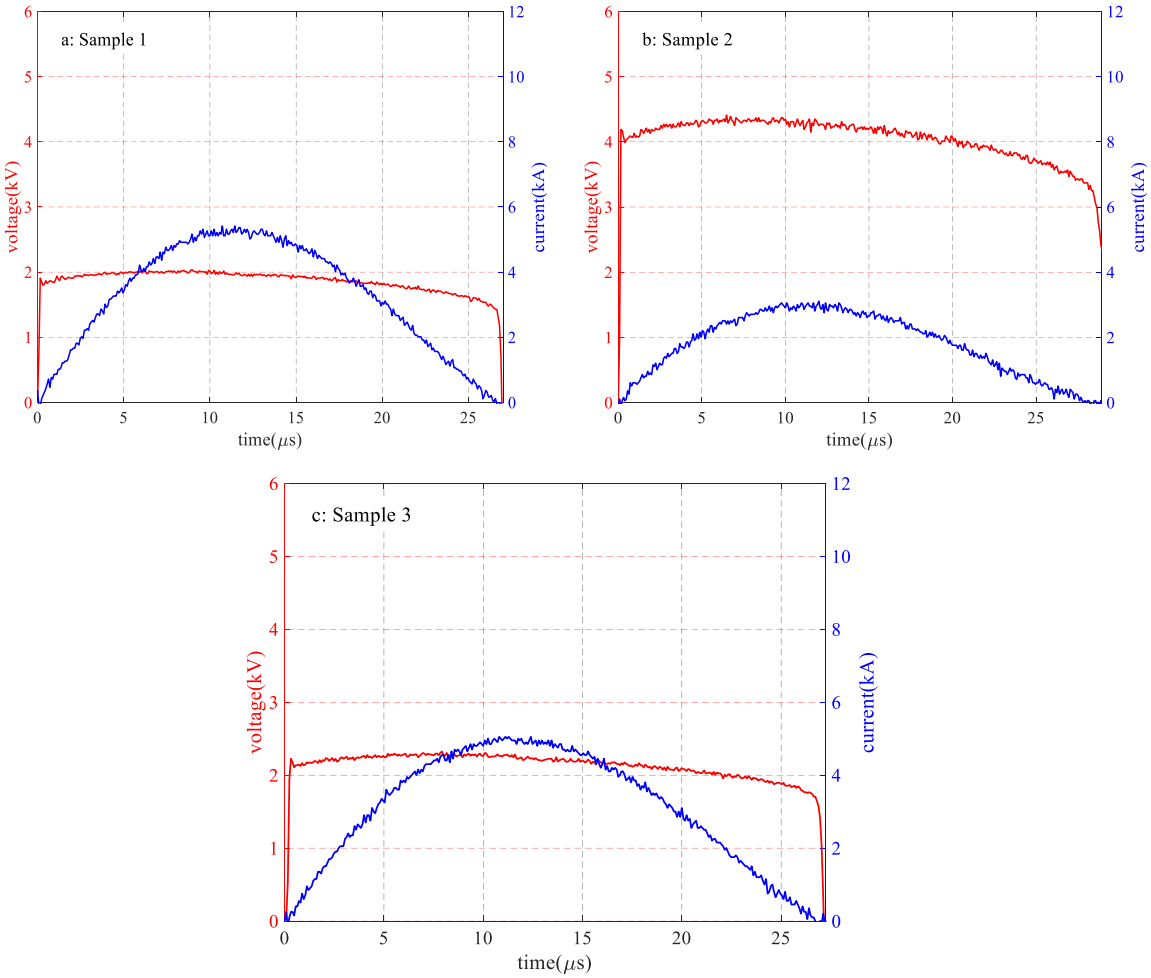

Figure 2-7: Typical impulse current and voltage for different samples. Discharge current and residual voltage of three samples of MO varistors tested with same impulse source charged to 8 kV

This project has received funding from the European Union's Horizon 2020 research and innovation programme under grant agreement No 691714.

The above elaboration may not be sufficient to understand the impact of physical dimensions, yet a more precise and strict relationship between current and voltage of a varistor block is better described by an electric field and current density. The relationship is that the higher the electric field, the higher current density or vice versa (more detail in [4]). This can be seen from the impulse tests shown in Figure 2-7. From the dimensions of the varistor samples and considering the results shown in Figure 2-7, the electric field across sample 1 is 0.317 kV/mm. The electric fields across sample 2 and sample 3 are 0.254 kV/mm and 0.243 kV/mm, respectively. Now, the resulting current densities are 1.379 A/mm^2, 0.625 A/mm^2, 0.652 A/mm^2 through sample 1, sample 2 and sample 3. Thus, to achieve similar current density, equal electric field across the varistor blocks must be ensured. This will lead to different total current for varistors having different diameters.

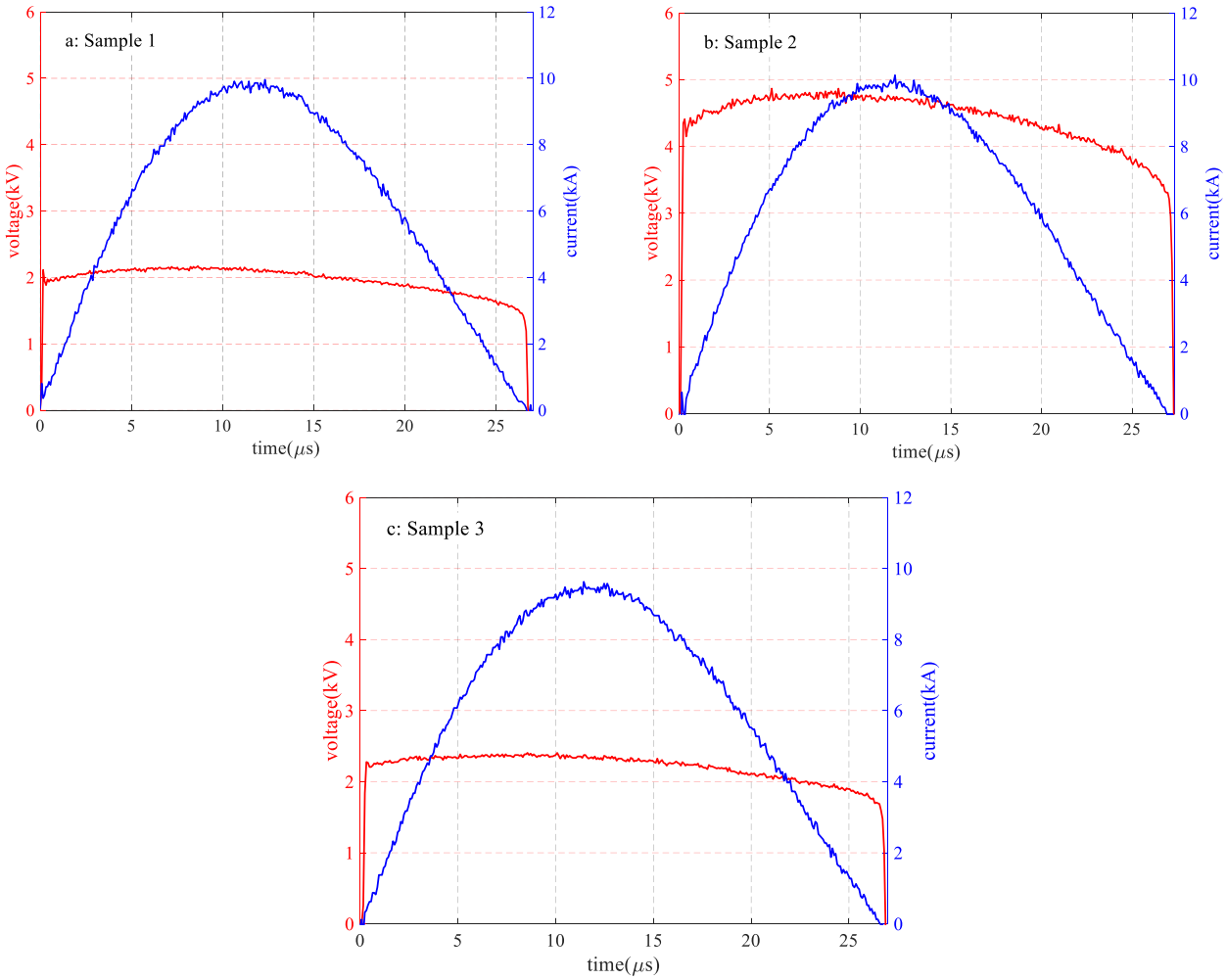

Figure 2-8: Typical residual voltages of different samples of MO varistors at 10 kA discharge current

Next, the focus is to obtain the same discharge current through each sample by varying impulse source voltage. Figure 2-8 shows the residual voltage of each varistor sample at approximately 10 kA discharge current. In this case the charging voltage of the impulse generator is adjusted to achieve the desired discharge currents. From

This project has received funding from the European Union's Horizon 2020 research and innovation programme under grant agreement No 691714.

this figure, the residual voltage of a given sample is proportional to its height. Thus, sample 1 has residual voltage of 2.14 kV, sample 2 has residual voltage of 5.14 kV and sample 3 has residual voltage of 2.39 kV (although the discharge current of sample 3 is slightly lower than 10 kA). The resulting current density through each varistor block, sample 1, sample 2 and sample 3 is, 2.558 A/mm^2, 2.078 A/mm^2 and 1.254 A/mm^2, respectively. Now the resulting electric field also follows the similar pattern as current density with the highest electric field being across sample 1 since it has the highest current density. Thus, the electric field across each sample at 10 kA discharge current is 0.338 kV/mm, 0.279 kV/mm, and 0.253 kV/mm. The main conclusion from the above discussion is that two varistor blocks cannot have identical I-V characteristics unless both have identical dimensions.

In addition to the above results, several impulse tests have been performed in order to investigate the impacts of the dimensions of varistor samples. Table 4 summarizes measurement results of several impulse tests of the three samples. These measurement results further justify the above discussion.

Table 4: Measurement of impulse current and voltage across sample 1 MO varistor under different source voltage – temperature and energy are included. Please describe the symbols. Use comma or dot as decimal separator, not both.

Sample 1							
Shot No.	û /kV	î /kA	T1 /µs	T2 /µs	Temperature /°C	Source voltage /kV	energy /kJ
1	1,903	2,609	9,1	20,16	27.2	5	0,08006
2	2,01	5,29	8,90	20,88	27.5	8	0,17
3	2,13	9,70	9,40	20,96	28.1	13	0,34
4	2,14	9,81	9,30	21,52	-	13	0,35
5	2,13	9,76	9,10	21,04	-	13	0,34
6	2,20	9,80	9,10	21,12	-	13	0,35
7	2,14	9,77	9,00	20,80	-	13	0,34
8	2,14	9,80	9,40	20,80	33.8	13	0,34
Sample 2							
19	4,26	0,62	16,10	17,44	26.7	5	0,05
20	3,99	3,01	11,70	20,88	29.5		0,20
21	4,68	2,98	9,00	20,88		8	0,24
22	5,01	7,19	9,10	20,72	30.7	13	0,58
23	5,07	8,96	8,80	20,88	31.9	15	0,74
24	5,14	9,91	9,20	20,80	36.2		0,82
25	5,17	10,23	9,00	21,04			0,86
26	5,14	9,99	9,50	21,04	-	16.2	0,83
27	5,16	9,99	9,30	20,72		16.2	0,83
28	5,16	10,15	9,00	20,96	-	16.2	0,86
29	5,18	9,99	8,90	20,80	-	16.2	0,84
30	5,14	9,95	9,70	20,96	-	16.2	0,83
31	5,18	9,95	9,20	20,64	42.1	16.2	0,84
Sample 3							

This project has received funding from the European Union's Horizon 2020 research and innovation programme under grant agreement No 691714.

9	2,19	2,97	9,40	20,32	-	Flash over (small gap distance)	0,11
10	2,21	3,31	9,60	20,48	-	Flash over (small gap distance)	0,12
11	2.17	2.401	10.50	20.72	27.5	5	0.09
12	2,29	5,00	9,80	21,12	27.8	8	0,18
13	2,39	9,62	9,20	20,88	28.5	13	0,37
14	2,37	9,45	9,30	20,80	-	13	0,36
15	2,39	9,45	9,20	21,12	-	13	0,37
16	2,40	9,45	8,80	21,12	-	13	0,37
17	2,38	9,48	9,30	20,96	-	13	0,37
18	2,40	9,44	9,00	20,88	32.3	13	0,37

Another important information from the I-V characteristics of a metal oxide varistor is the leakage current under normal system condition. See the pre-breakdown region in Figure 2-4. It must be noted that for HVDC circuit breaker application this characteristic does not play a significant role since under normal system operation condition the MOSA branch is short-circuited by the main current path. Thus, the MOSA branch will not see a system voltage and hence no leakage current and no thermal stress. However, in most HVDC circuit breakers the MOSA branch sees the system voltage right after current interruption until the residual current breaker opens. This step follows just after the MOSA has absorbed the system energy. At this stage the MOSA could be at high temperature due to the absorbed energy and if the residual current breaker is not opened quickly, the subsequent leakage current may lead to unnecessary aging/thermal run away or even failure of the MOSA branch.

a) b)

Figure 2-9: A set-up for measurement of the I-V characteristics of an MO varistor at different temperatures i.e. test set-up in an oven (for temperature control)

As shown in Figure 2-4, the I-V characteristics in the leakage current region strongly depend on the temperature of the MO varistor. The higher the temperature the larger the leakage current at a specific voltage. Thus, if the HVDC circuit breaker is not quickly isolated from the system by a residual current breaker, it could lead to potential thermal run away. The magnitude of leakage current depends also on the type of source (AC or DC) and the

This project has received funding from the European Union's Horizon 2020 research and innovation programme under grant agreement No 691714.

temperature of the varistor blocks. Figure 2-9 shows test set-up for measuring leakage current of a varistor block. Normally, this test is set-up in an oven to investigate the impact of temperature on leakage current levels. Figure 2-10 shows typical leakage current region (pre-breakdown) of a varistor block under a DC voltage source.

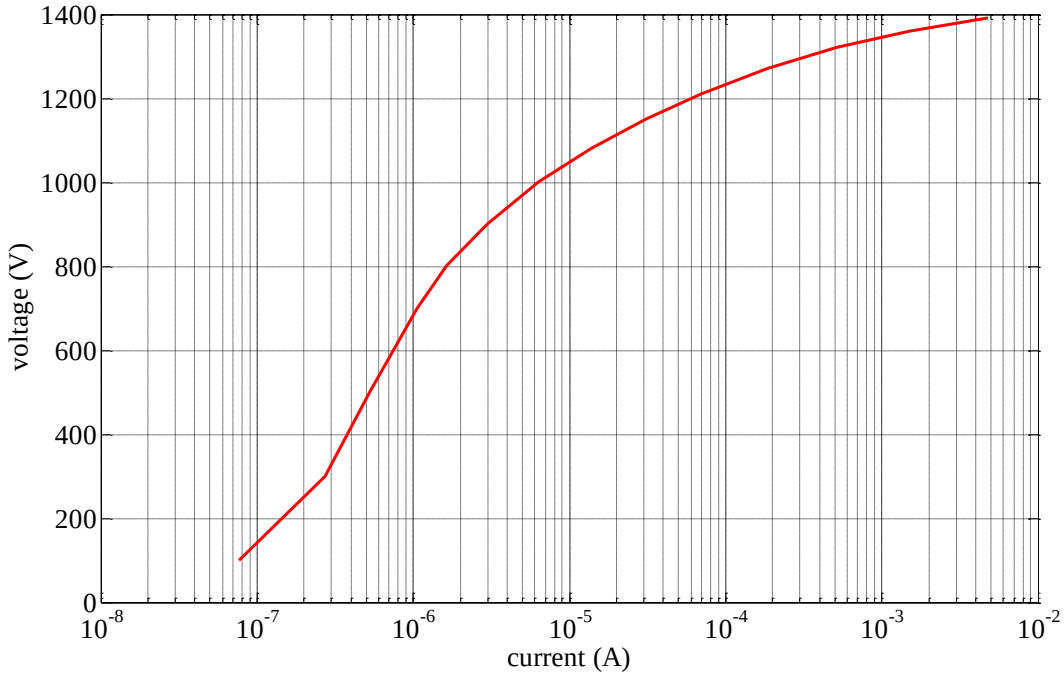

Figure 2-10: Measurement of I-V characteristics (DC) of MO varistors in the leakage current region (at 25.67 ºC and 44.92% humidity level)

2.2.2. SPECIFICATION OF METAL OXIDE VARISTOR BLOCKS FOR EXPERIMENTAL DC CB

The maximum varistor block size that can be manufactured is limited; for example, 20 to 45 mm in height [4] and 38 to 108 mm in diameter [5]. This means several varistor blocks must be used in series and in parallel for high voltage and large energy absorption requirements, respectively.

For HVDC circuit breaker application, several columns of varistor blocks are needed to handle large amount of energy. Given a specific energy requirement, the number of varistor blocks needed depend on the energy per volume that can be injected to a varistor block for a safe operation. These varistors need to be arranged in several columns while taking the residual voltage of columns into account. In order to limit the number of columns, the larger size (diameter) varistor blocks are preferable. The procedure for designing MOSA for HVDC circuit breaker and column matching are discussed in the proceeding sections. Figure 2-11 shows the varistor block used to build the MOSA branch of the experimental DC CB.

For the purpose of experimental DC CB in this project, a varistor blocks with the following specification are used. The MO varistors would be SIEMENS/EPCOS Type E99NR702D (D stands for DC stable), variant S051 with following technical data:

- diameter: 99 mm +/-1,0 mm

This project has received funding from the European Union's Horizon 2020 research and innovation programme under grant agreement No 691714.

- height: 21,4 mm +/- 0,6 mm
- repetitive charge transfer rating, Qrs: 6,0 As (2ms) – the maximum charge transfer capability in one event. Arrester is required to handle at least 20 of such an event without failure.
- I 4/10: 100 kA – lightning impulse current of 100 kA with 4 µs rise time and 10 µs tail (to 50 %)
- Residual voltage (U_{res}) at 10kA, 8/20 lightning impulse: 7,5 kV - The residual voltage across the varistor when 10 kA, 8/20 lightning impulse current is flowing.

Figure 2-11: Photo showing ratings of a MO-varistor disk used in the experimental DC CB. The label shows residual voltage of 7.39 kV at 10 kA discharge current

The I-V characteristics of the chosen varistor is shown in Figure 2-12. In this figure, temperature as well as source type dependency of leakage current is included. In addition to the current magnitude the residual voltage across the varistor is dependent on the rate of rise of impulse current. The higher the rate of rise of impulse current, the higher the residual voltage, see the curves for 1/2 µs, 8/20 µs and 30/60 µs impulses in the high-current region.

This project has received funding from the European Union's Horizon 2020 research and innovation programme under grant agreement No 691714.

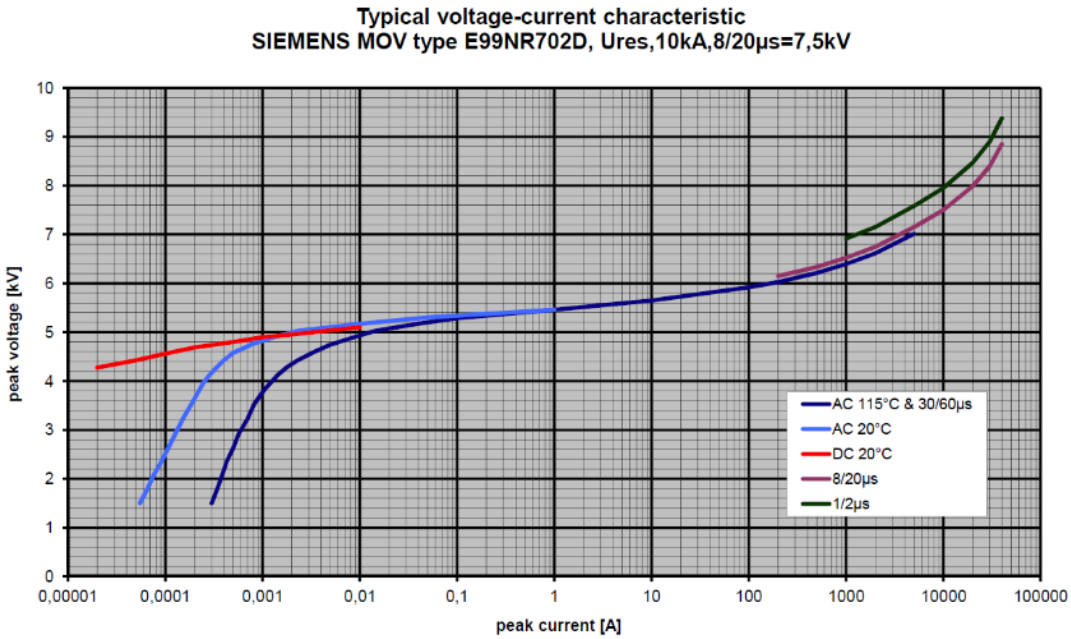

Figure 2-12: I-V characteristics of metal oxide resistor used in the experimental DC CB (SIEMENS)

2.2.3. DESIGN OF MOSA COLUMN FOR EXPERIMENTAL DC CB

The main interrupter of the experimental DC CB is a vacuum circuit breaker with rating described in Section 2.1. The voltage rating of a single phase of these VCBs is in the range of 38-40 kV (rms, for AC application). In order not to exceed the AC voltage ratings, the equivalent voltage for the experimental DC CB is chosen to be 40 kV with overshoots as high as 45 kV.

That means, during the current interruption process, the TIV of the experimental DC CB shall not exceed 45 kV. From the I-V characteristics of the chosen varistor (see Figure 2-12) the voltage at 10 kA discharge current for a single varistor is 7.5 kV. This results in six varistors in series to meet 45 kV TIV requirement. The design of a single column with special features and dimensions is shown Figure 2-13.

This project has received funding from the European Union's Horizon 2020 research and innovation programme under grant agreement No 691714.

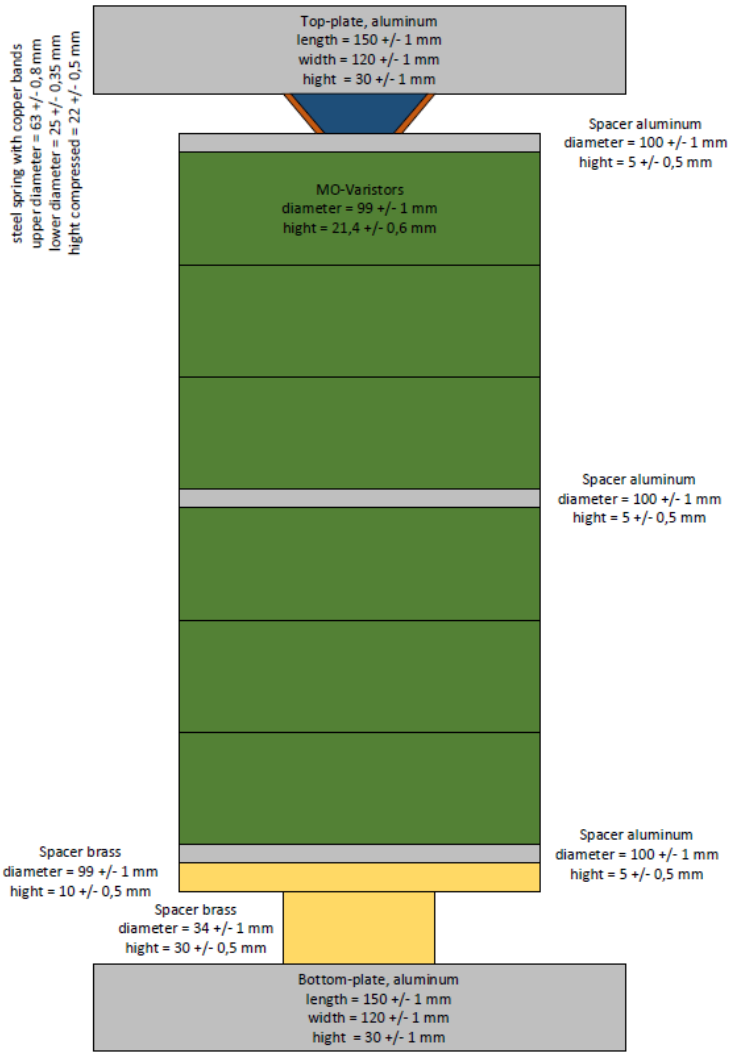

Figure 2-13: Design of a single column of MOSA for experimental DC CB

In the design shown, three aluminium spacers are used; top, middle and bottom. Top and bottom spacers are needed to provide good electrical contact throughout the surface of the upper side of the top disc and lower side of the bottom surface, to ensure uniform current distribution throughout the surface of the varistor.

Part of the investigation on the experimental DC CB is on the MOSA branch, for example, thermal energy handling, current sharing among multiple columns, etc. For this reason, transient current through multiple columns as well as real-time temperature of several columns is monitored during the interruption process. Access for these measurements have been included in the MOSA column design shown in Figure 2-13. The aluminium spacer in the middle is needed to gain access to temperature measurement. It is pierced in the radial direction up to the centre for placing fibre optic-based temperature sensor probes. For current measurements a brass spacer at the bottom is provided. The brass spacer has smaller diameter than the varistor blocks to allow winding Rogowski current sensors around.

This project has received funding from the European Union's Horizon 2020 research and innovation programme under grant agreement No 691714.

Moreover, since the experimental DC CB is tested in indoor environment, there is no need to put the varistor columns in insulators. This of course has an impact on the cooling down time after energy absorption. In addition, columns are arranged in such a way that the surface temperature of each column can be monitored from each side by a thermal camera.

2.2.4. DESIGN PROCEDURE OF MOSA FOR HVDC CIRCUIT BREAKER APPLICATION

For designing the MOSA branch for HVDC circuit breaker application, the following parameters must be specified. These parameters are described below.

1. **Transient Interruption voltage (TIV)**: - corresponds to residual voltage at rated interruption current. This is determined by the height of the active part (length of varistor column). To suppress the fault current, this voltage must be higher than the system nominal voltage for which the breaker is designed. So far, a factor of 1.3 -1.5 is assumed to be sufficient.
2. **Current**: - the range of current from load to the rated interruption current of the HVDC circuit breaker must be specified. This combined with the cross-sectional area of the active part has an impact on the TIV that can be generated during current interruption.
3. **Energy**: - The maximum energy that the MOSA can absorb without mechanical/electrical degradation. The volume of the active part determines the maximum energy absorption capability. Although it is mentioned in the literature that energy up to 400 J/cm^3 can be injected to MOSA, energy of 200 J/cm^3 during single absorption period is considered to be safe for reliable and durable service. The MOSA can operate reliably in a temperature range of 100 to 300 ºC. Typically, for energy of 3.3 J/cm^3, the MOSA temperature increases by about 1 ºC. Thus, 200 J/cm^3 energy injection results in temperature increase of about 61 ºC.

As discussed in the previous section, current and voltage are related to one another through electric field and current density. The higher the current density, the higher the electric field. Thus, when designing multi-column MOSA, this fact must be considered since at a given rated current the higher the number of columns, the lower the current density and hence the lower the residual voltage.

For a single break experimental DC CB, the following parameters are specified

- Rated interruption current 20 kA (this is considering sufficient margin)
- Rated energy 2 MJ
- TIV 40-45 kV

Considering the above parameters, the design of MOSA (made of the varistors specified in the previous section) which can fulfil these requirements can be determined as follows.

The volume of MOSA needed to handle the specified energy (assuming 200 J/cm^3) is,

This project has received funding from the European Union's Horizon 2020 research and innovation programme under grant agreement No 691714.

$$V = \frac{2 * 10^6\ J}{200\ J/cm^3} = 10000\ cm^3$$

The number of varistor disks (with dimensions specified in the preceding section) needed to meet this volumetric requirement is 60. To meet the TIV requirement, 6 varistors in series have, 45 kV residual voltage at 10 kA[2] discharge current. Thus, the 60 varistors need to be arranged in 10 columns. It must be noted that to get 45 kV residual voltage out of 10 columns, the injected current must have a peak value of 100 kA. However, the peak value of interrupted current is specified to be 20 kA. This corresponds to 2 kA current per column. From the I-V characteristics of the varistor shown in Figure 2-12, the residual voltage at 2 kA per varistor disk is 6.8 kV. This makes the residual voltage of the entire MOSA stack 40.8 kV. The design of the MOSA for experimental DC CB is shown in Figure 2-14.

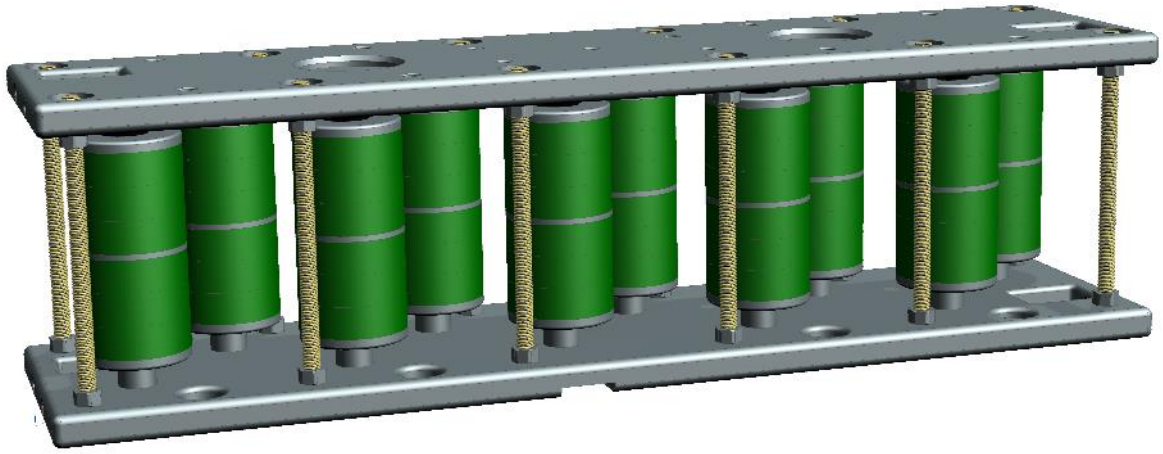

Figure 2-14: Design of MOSA stack for experimental DC CB

Note that the residual voltage of 40.8 kV corresponds to the TIV that appears when interrupting DC current of 20 kA. Another important point to note is the residual voltage of the same MOSA stack when interrupting low current, for example, high-impedance fault current or even load current. For instance, considering 2 kA load current interruption, the DC breaker still needs to produce a TIV higher than the system voltage. For instance, during load current interruption the DC breaker pushes 2 kA load current into the MOSA branch. The corresponding residual voltage (the TIV) of MOSA can be found from Figure 2-12, where 200 A is flowing through a single column[3] is 36 kV. As discussed in the previous sections, the reduced TIV is due to the reduced current density through the varistors when interrupting low currents. This is the main reason that the fault current suppression time for high current and low current remain more or less equal although there is significant difference in the energy absorption [6] [7]. This will be elaborated later in subsection 2.2.6.

[2] This is assuming 8/20 impulse current. In reality the final value of the residual voltage depends on the steepness of the current being injected into the varistor. In DC circuit breaker application, the rate of rise of current being pushed to the MOSA is lower than 8/20 impulse current and thus the resulting TIV is slightly lower than the values presented here.
[3] Assuming equal current sharing among the 10 columns. For this assumption to be valid the columns must be checked for matching I-V characteristics.

This project has received funding from the European Union's Horizon 2020 research and innovation programme under grant agreement No 691714.

2.2.5. MOSA COLUMN MATCHING

From the discussion in the earlier subsections, a single stack of MOSA to be used with one vacuum interrupter has 10 columns (later two columns are added as safety margin for energy and thus, 12 columns). Each column consists of six varistor blocks each of which has (nearly) identical I-V characteristics. However, when combining the varistors into columns, it is (practically) impossible to have two or more of these columns with matching I-V characteristics. Obviously, if the columns do not have (nearly) identical I-V characteristics, equal current sharing and hence, equal energy absorption cannot be guaranteed. This is not desirable since it leads to unequal heating of the columns or even breakdown of the stressed columns. Therefore, before assembling the MOSA stack, it is necessary to ensure each of the columns have I-V characteristics within acceptable range. This can be achieved by performing the column matching procedure which is discussed below.

Before the actual column matching procedure, one column is chosen to serve as a reference column against which the other columns are compared. The matching procedure is performed by applying 8/20 µs impulse to the parallel arrangement of several columns in which one is the reference column. Then, the resulting impulse current flowing through each column is compared against the impulse current through the reference column. In order to facilitate the matching procedure, first, each of the columns are arranged/pre-sorted based on the total sum of the residual voltage (voltage at 10 kA discharge current labelled by manufacturer) of the varistors constituting the columns. Considering the residual voltage printed on the varistor blocks, there are 10 sets of varistors with residual voltage ranging from 7.35 kV to 7.44 kV, i.e. at steps of 10 V as shown in Figure 2-15. Thus, these varistors are combined and arranged into six groups as shown in Table 5. As can be seen from this table, the columns are built in such a way that the total sum of the residual voltages of each column is equal (44.37 kV).

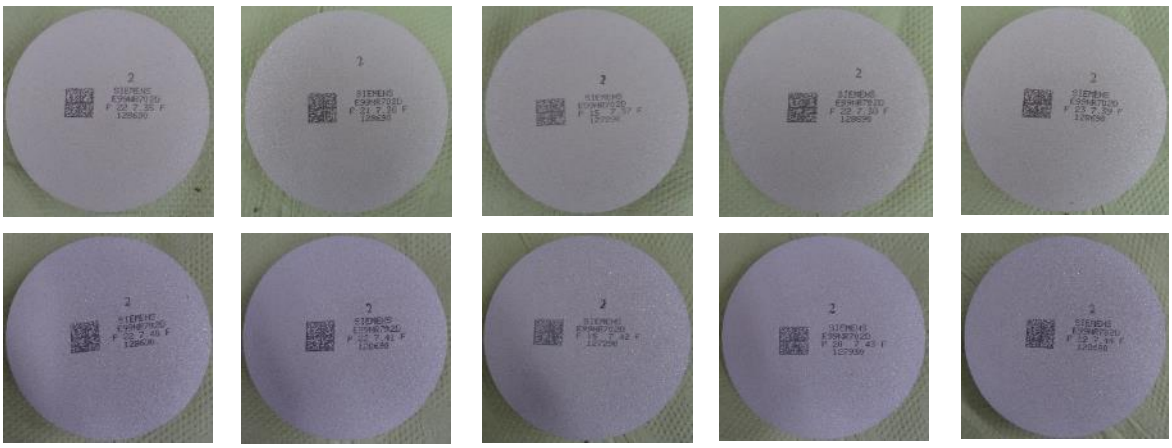

Figure 2-15: Ten metal oxide varistor blocks with slightly different residual voltage (ranging from 7.35 – 7.44 kV)

Table 5: The residual voltages of varistors constituting pre-sorted columns based on the information labelled on the varistors

MO Resistors	Column 1	Column 2	Column 3	Column 4	Column 5	Column 6

This project has received funding from the European Union's Horizon 2020 research and innovation programme under grant agreement No 691714.

1	7.35	7.36	7.35	7.36	7.35	7.35
2	7.38	7.38	7.37	7.37	7.36	7.37
3	7.39	7.39	7.38	7.39	7.38	7.39
4	7.40	7.40	7.41	7.40	7.41	7.40
5	7.41	7.41	7.42	7.42	7.43	7.42
6	7.44	7.43	7.44	7.43	7.44	7.44
Total	44.37	44.37	44.37	44.37	44.37	44.37

Figure 2-16 shows the varistors constituting one column shown Table 5 (specifically column 5). Then, the pre-sorted varistors are arranged as shown in Figure 2-17.

.

Figure 2-16: six MO-varistor discs making one column of the MOSA stack

This project has received funding from the European Union's Horizon 2020 research and innovation programme under grant agreement No 691714.

Figure 2-17: Several columns arranged for matching based on pre-sorted MO-varistor blocks. The total sum of the residual voltages All these columns have equal total sum of residual voltages.

As mentioned before, pre-sorting based on residual voltage of varistors does not guarantee matched I-V characteristics of columns. Matching can only be confirmed after testing for current sharing among columns. A test set-up of the matching procedure is shown in Figure 2-18. Six columns, one of which is a reference column, are compressed between two aluminium plates as shown in the figure. It must be noted that all the six columns should be compressed equally. Note that matching can be performed on more than six columns at a time provided that the test set-up can accommodate more columns.

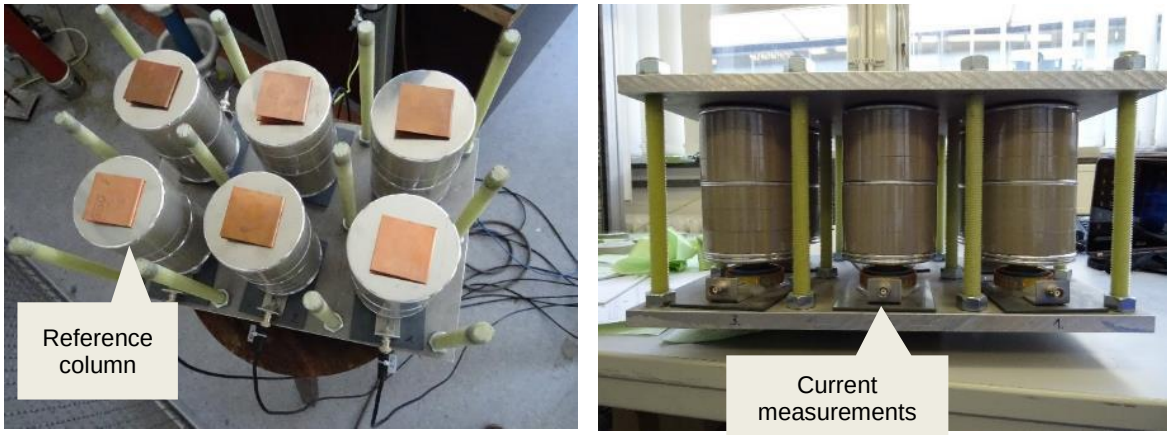

Figure 2-18: Arrangement of MO-varistor columns during the matching test

This project has received funding from the European Union's Horizon 2020 research and innovation programme under grant agreement No 691714.

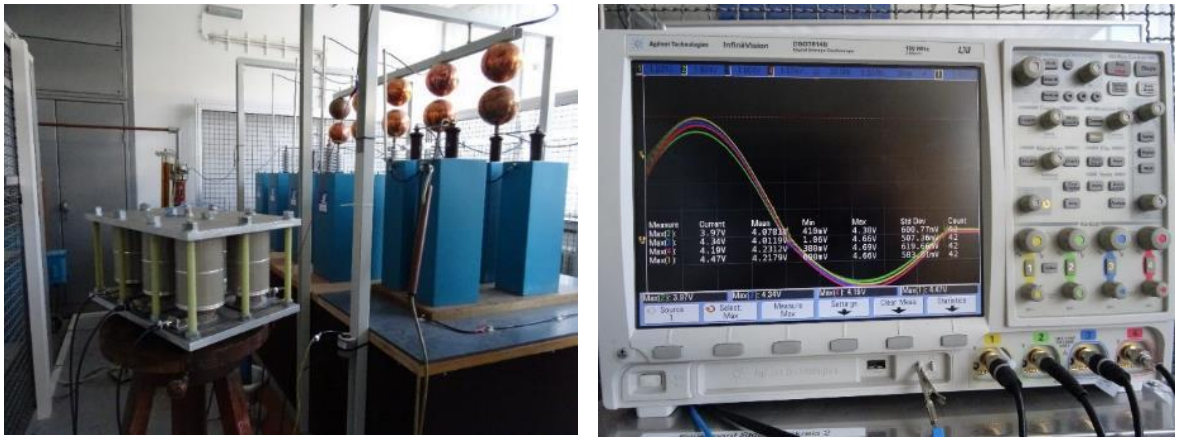

Figure 2-19: Typical oscilloscope reading during the column matching procedure. Channel 3 (blue) is the reference column

Then, 8/20 µs impulses are successively applied to the entire arrangement so that 10 kA impulse current is shared between the six columns. Current flowing through each column is measured. For example, typical impulse current through each column is shown in Figure 2-20. Here again for comparison purpose it suffices to compare only the peak values of the currents through the columns. Up to 20 impulse shots are needed until stable/repeatable impulse current is measured. After performing 20 shots, the measurements from the last two shots are compared against the current measurement through the reference column. The matching criterion is set such that the columns with current measurement falling within ±5 % of the current measured through reference column are considered as matched. Note here that the matching criterion could be increased or decreased if necessary. Nevertheless, the tighter the matching criteria, the better.

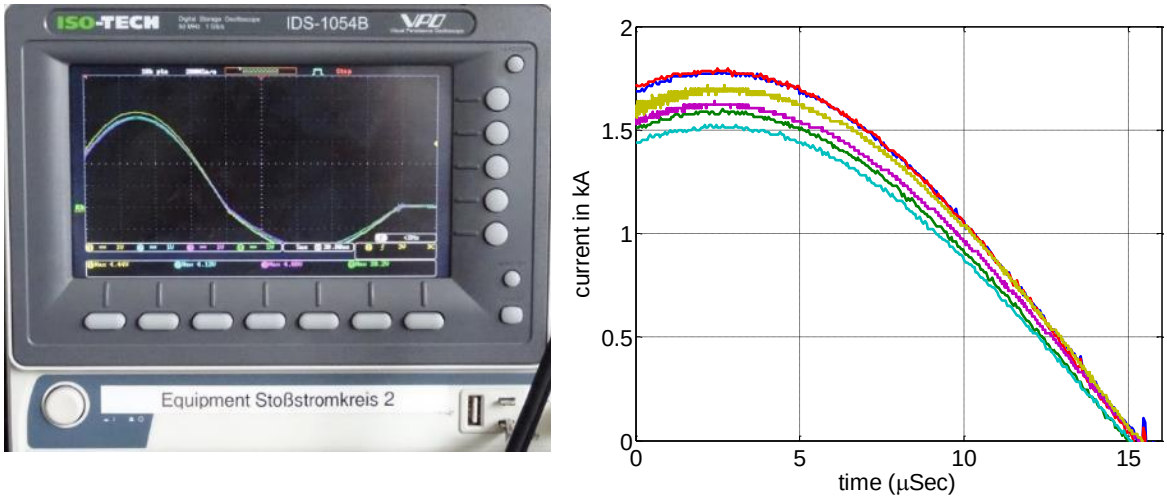

Figure 2-20: Typical impulse current measured through six columns

An example case of impulse current measurements through each column during the matching procedure is shown in Table 6. In this table, current measurement of only 10 successive impulses are depicted. For comparison purpose it is enough to consider only the peak values of the measured currents. For matching, the last two rows of Table 6 are considered. Thus, the measurements are compared against the reference column (column 4 in this

This project has received funding from the European Union's Horizon 2020 research and innovation programme under grant agreement No 691714.

case).This can be seen from Table 6 where column 2 and column 6 pass the matching criterion while column 1, 3 and 5 do not meet the matching criterion. Therefore, the varistors in column 1, 3 and 5 are rejected and must go through another matching process. Before going through the next phase of matching procedure, a few varistor blocks of these columns need to be swapped to adjust the residual voltage. Considering the rejected columns, all of these columns draw larger current than the reference column. In other words, these columns have lower residual voltage compared to the reference column. Thus, the residual voltage of these columns need to be adjusted by replacing a varistor block having lower residual voltage (e.g. 7.35 kV) with a varistor with higher residual voltage (e.g. 7.38 kV).

Table 6: An example case impulse current measurement of six columns to demonstrate the matching procedure

Shot no.	Column 1	Column 2	Column 3	Column 4 (reference)	Column 5	Column 6
1	4.56	4.09	4.59	3.91	4.64	4.00
2	4.47	4.13	4.50	4.97	4.48	4.08
3	4.44	4.16	4.56	4.03	4.48	4.08
4	4.41	4.19	4.41	4.03	4.44	4.12
5	4.44	4.19	4.44	4.03	4.44	4.12
6	4.41	4.19	4.50	4.06	4.44	4.12
7	4.41	4.19	4.50	4.06	4.44	4.16
8	4.38	4.19	4.38	4.06	4.44	4.12
9	4.41	4.22	4.38	4.06	4.36	4.16
10	4.34	4.19	4.38	4.06	4.40	4.12
select/reject	✗	✓	✗	3.857-4.263	✗	✓

Compare the last two rows

Increase reference voltage

Criteria ±5%

Increase reference voltage

The procedure continues until the needed number of matched columns are obtained for building a stack of MOSA. Figure 2-21 shows MOSA stack made of 12 matched columns.

Figure 2-21: MOSA stack with matched columns

This project has received funding from the European Union's Horizon 2020 research and innovation programme under grant agreement No 691714.

2.2.6. IMPACT OF NUMBER OF COLUMNS ON THE RESIDUAL VOLTAGE OF MOSA

In subsection 2.2.4 it is described that several varistor columns are needed to deal with the energy absorption requirement. However, this will have an impact on the TIV that can be generate by the DC CB during current interruption. In this section, experimental demonstration of various number of columns on the TIV that can be generated by HVDC circuit breaker is presented. It must be noted that increased number of varistor column means increased surface area and hence decreased current density. The discussion in this section follows and justifies what has been presented in subsection 2.2.1. In this section, impulse current of 10 kA is applied to 1, 2, 3 and 12 columns as shown in Figure 2-22.

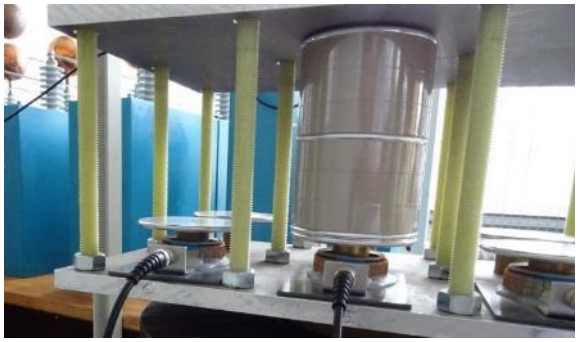

a) One column

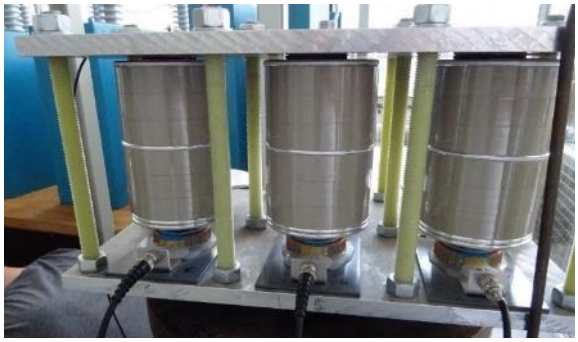

b) Three columns

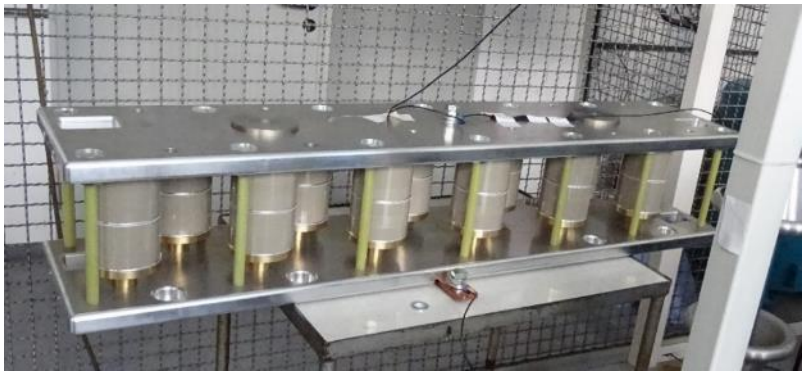

c) 12 columns

Figure 2-22: Test set-up for demonstration of the impact of number of columns on the residual voltage at 10 kA source current

Figure 2-23 shows residual voltage measurement (left y-axis) across and current measurement (right y-axis) through a single column of varistor blocks. The peak value of the impulse current is 10 kA. At peak current (at T on x-axis) the residual voltage measured is 47.8 kV. Similarly, 10 kA impulse current is applied to two, three and 12 columns of varistor blocks. The resulting residual voltage is shown in Figure 2-24. It can be seen from this figure that as the number columns increase, the residual voltage decreases.

PROMOTiON – Progress on Meshed HVDC Offshore Transmission Networks

This project has received funding from the European Union's Horizon 2020 research and innovation programme under grant agreement No 691714.

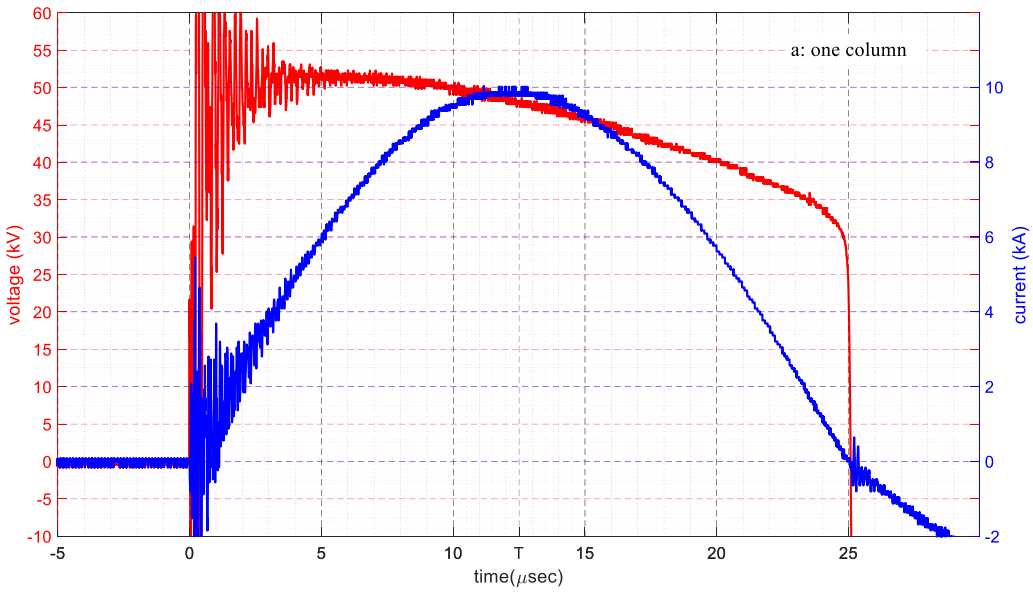

Figure 2-23: 10 kA impulse current and residual voltage across one column of MOSA (same as the blue trace in fig. 2-24)

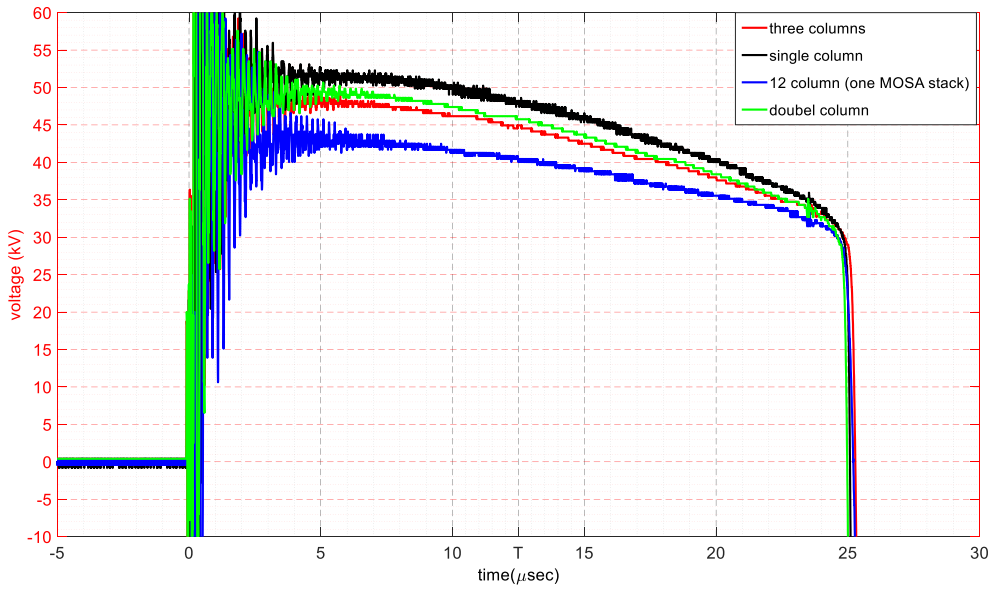

Figure 2-24: Comparison of residual voltage across various number of varistor columns when 10 kA source current is applied.

As discussed in section 2.2.1, at given current when the surface area of the varistors increase, the current density decreases and hence, the resulting electric field. Thus, when 10 kA impulse current flows through two columns, the current density through one column is halved. Since the varistor is operating in breakdown region the decrease in electric field is not linearly proportional to the decrease in current density. Note that, all the columns have equal height. This means equal electric field through a column lead to equal residual voltage. Similarly, for three and 12 columns case, the 10 kA impulse is shared among three columns and 12 columns, respectively, and the current densities in each case are reduced proportionally.

PROMOTiON – Progress on Meshed HVDC Offshore Transmission Networks

This project has received funding from the European Union's Horizon 2020 research and innovation programme under grant agreement No 691714.

2.3 SPECIFICATION OF THE INSTRUMENTATION SYSTEM

In order to quantify the stresses on various sub-components of HVDC circuit breaker, several quantities are measured and analysed. Besides, standard current through and the voltage across the entire test object, various current and voltage across internal sub-components are measured. In addition, temperature of MOSA columns during and after current interruption is measured. In this section specification of special measurements is described.

2.3.1 CURRENT MEASUREMENT

Referring to Figure 2-1, the following current measurements are performed.

- Total current flowing into the test object
- Current through the vacuum interrupter
- Current through the injection branch
- Current through the MOSA branch

In addition to the current through the vacuum interrupter, the rate of change of current through the vacuum interrupter and the initial voltage across the interrupter(s) is measured at very high frequency (bandwidth 20 MHz) with HBM HV6600 optically isolated data acquisition system with a sampling frequency of 100 MS/s for analysing ultra-fast “current zero” phenomena just before and after current interruption. For this a specially designed Rogowski coil is used.

In addition to the total current through the MOSA branch, current through individual columns are measured. Current through up to 8 columns is measured. This is later used for computation of energy dissipation per column and for comparison of current distribution/sharing through the columns as well. For measuring current through MOSA columns standard off-the shelf Rogowski coils, shown in Figure 2-25, with a slight modification are used.

Figure 2-25: Rogowski coil for measuring current through a MOSA column – PEM CWT30LFxB/4/300

This project has received funding from the European Union’s Horizon 2020 research and innovation programme under grant agreement No 691714.

The rogowski coils used for this purpose are designed to deal with electro-magnetic interference (EMI) in high-power/high-voltage environment. It is PEM CWT30LFxB/4/300 fitted with an integral electrostatic screen underneath the coil insulation to attenuate any unwanted electrostatic interference through capacitive coupling. It has the high frequency (-3 dB) bandwidth of approximately 2 MHz. The photo of the rogowski coil used for this purpose is shown in Figure 2-25.

The current through the MOSA branch is further analysed by measuring the current through individual MOSA columns. This is intended to investigate the current distribution among the MO-varistor columns since unequal distribution will lead to overheating of one column compared to the others. Current through up to 8 columns will be measured at a time. This will be supported by temperature measurement at the middle point of the individual columns

A. MEASUREMENT VERIFICATION

Before the use of the newly bought Rogowski current sensors, measurement verification test was performed under real power condition. The test set-up is shown Figure 2-26 where four Rogowski coils measure the same current. The measurement result current with peak value of nearly 3 kA is shown in Figure 2-27. The difference between the measurements of the four Rogowski coils is less than 1%.

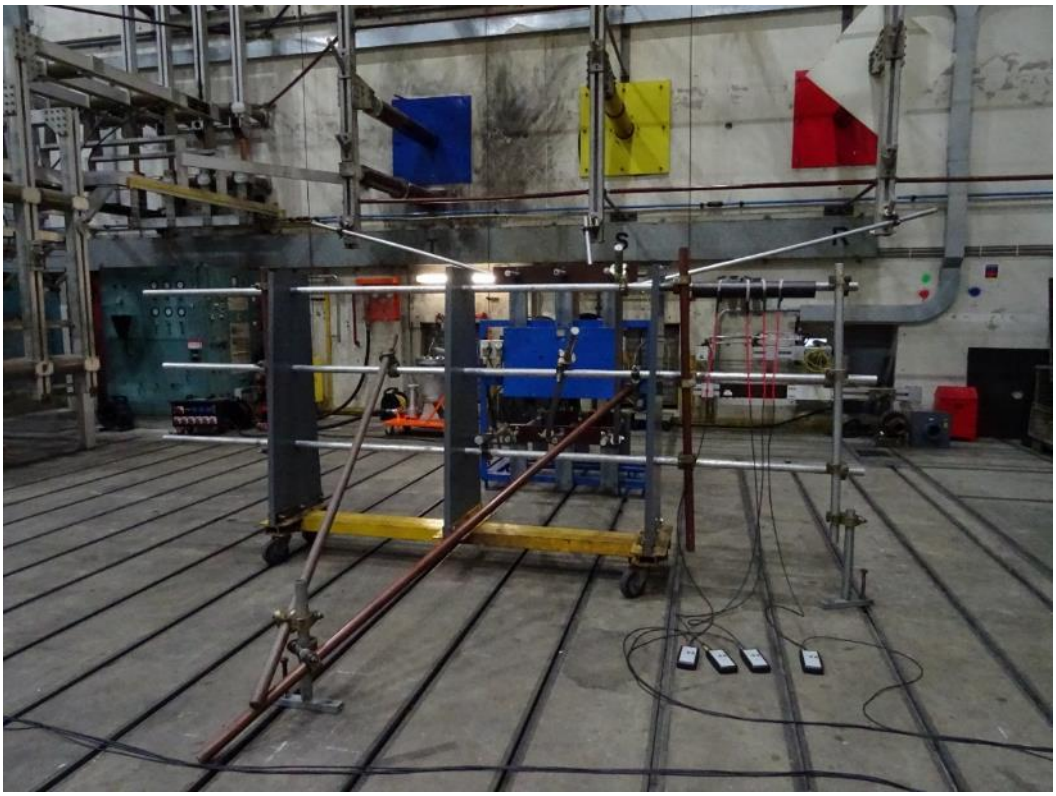

Figure 2-26: Verification of current measurement by Rogowski coils

This project has received funding from the European Union's Horizon 2020 research and innovation programme under grant agreement No 691714.

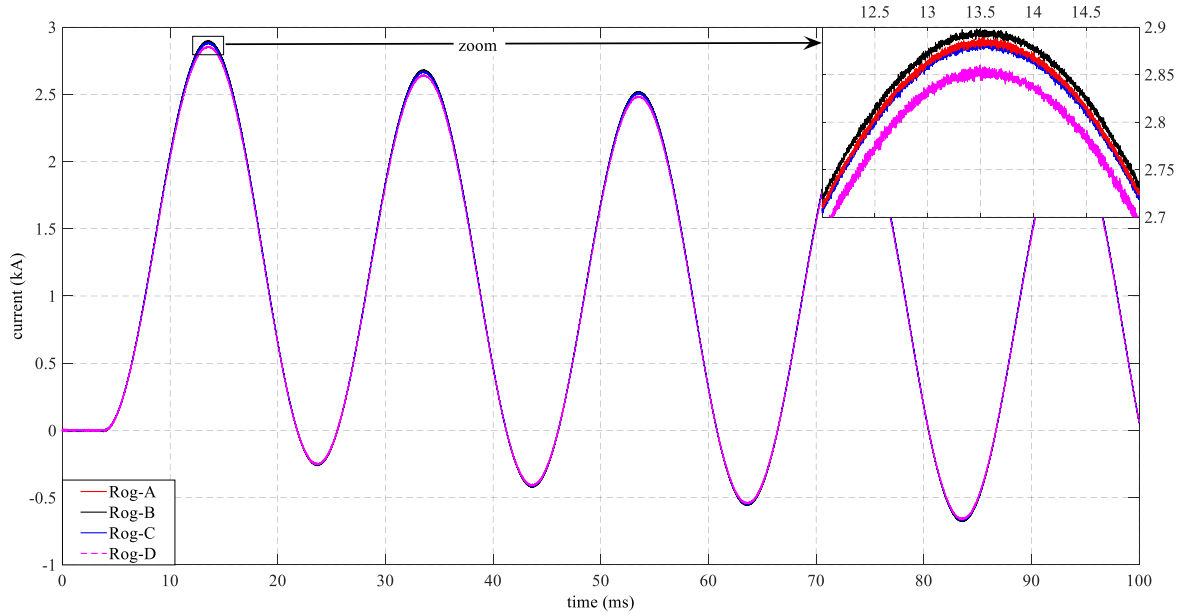

Figure 2-27: comparison of current measurements by four Rogowski current sensors. All the Rogowski current sensors have the same peak current (3 kA) capability.

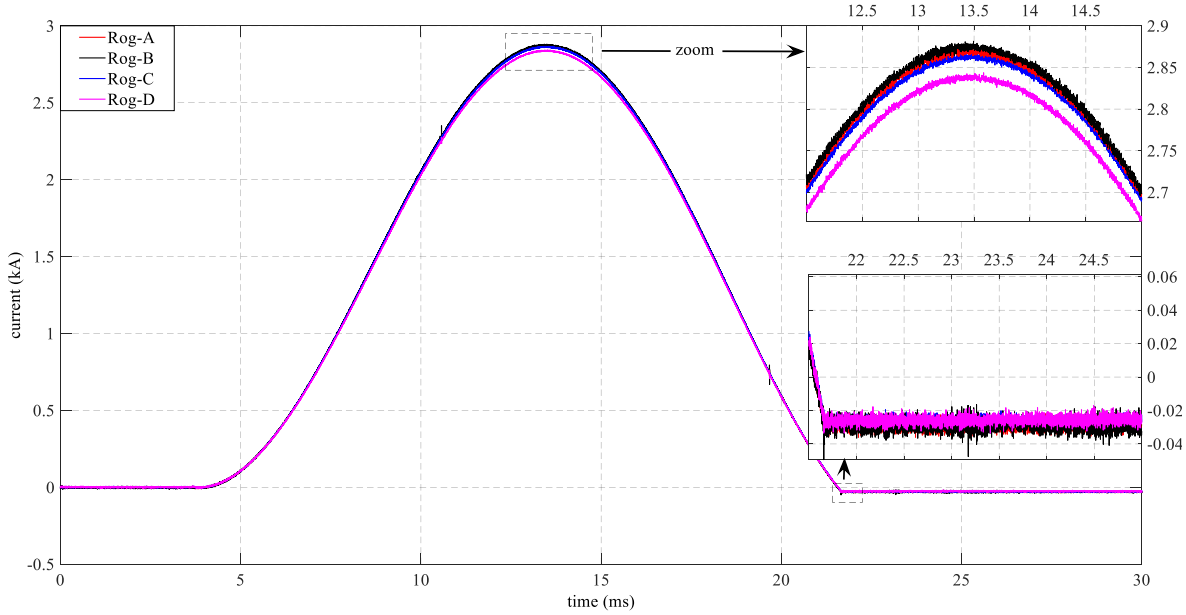

Figure 2-28: One loop current measurement by Rogowski current sensors.

Figure 2-28 shows a single loop AC current measurement by four Rogowski coils. Due to inherent behaviour of Rogowski coils (integration), there is a slight DC offset at the end of the loop. This need to be compensated for.

PROMOTiON – Progress on Meshed HVDC Offshore Transmission Networks

This project has received funding from the European Union's Horizon 2020 research and innovation programme under grant agreement No 691714.

B) CURRENT MEASUREMENT ON HIGH POTENTIAL

In some cases, the Rogowski current sensors are required to measure current on a floating potential, especially when two or more experimental vacuum interrupters are put in series for high voltage rating. In order to verify the performance on floating potential, test is set up with circuit shown in Figure 2-29

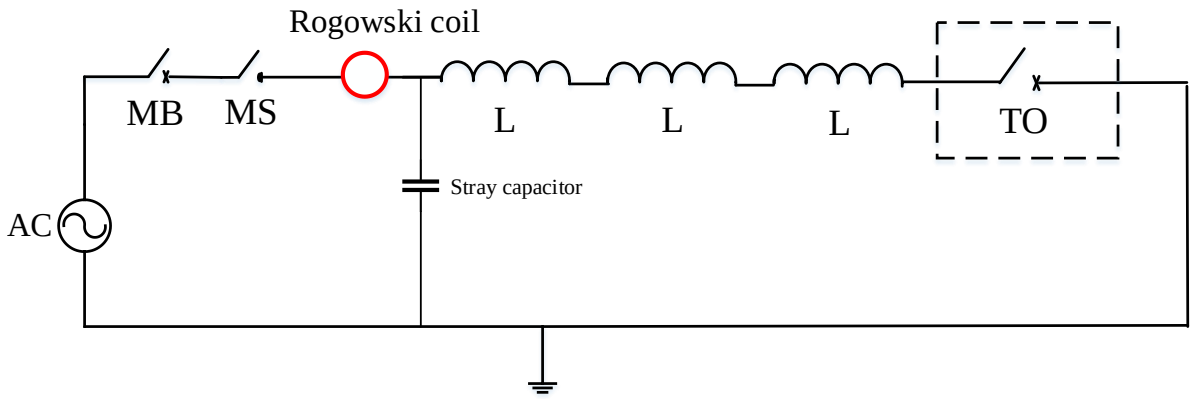

Figure 2-29: Circuit diagram showing test set-up for Rogowski current sensor on floating potential. (Stray capacitance is from step-up transformers and long rails used in the circuit)

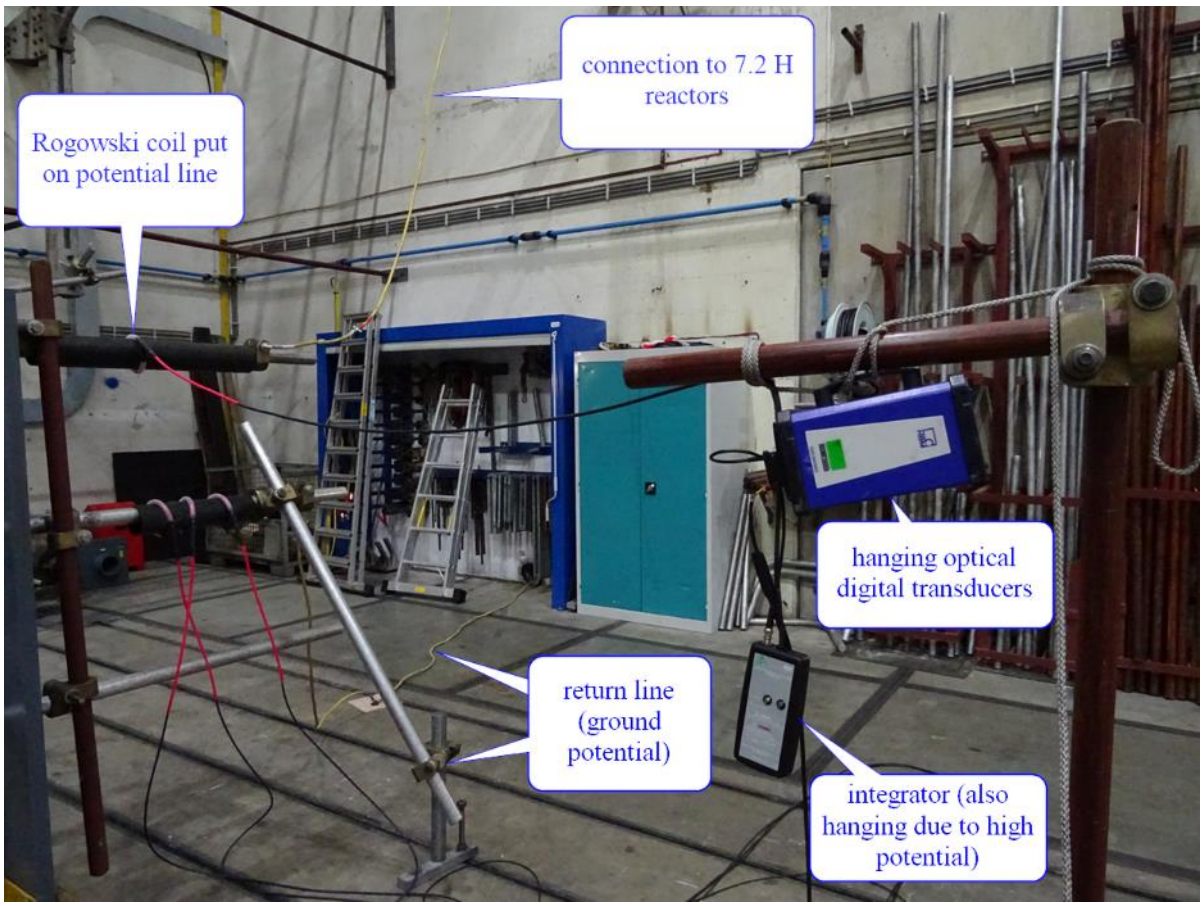

Figure 2-30: Current measurement on a high potential line by Rogowski current sensors

This project has received funding from the European Union's Horizon 2020 research and innovation programme under grant agreement No 691714.

Figure 2-31: Three reactors (2.4 H each) connected in series for low current measurement on high potential line

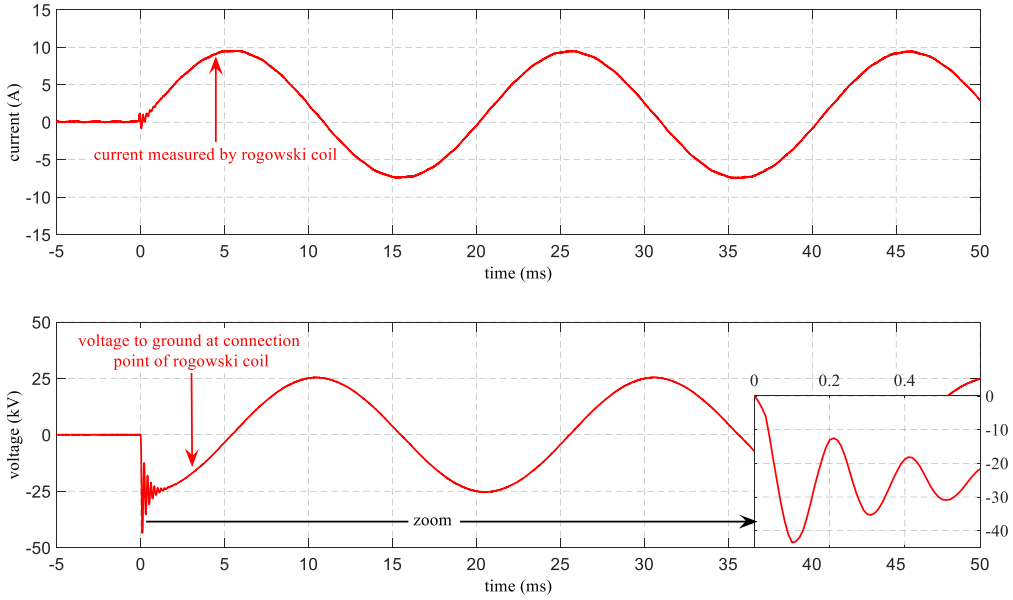

Figure 2-32: a) Measurement result by Rogowski current sensor on potential. b) voltage to ground at a point of current measurement by Rogowski current sensor

This project has received funding from the European Union's Horizon 2020 research and innovation programme under grant agreement No 691714.

2.3.2 VOLTAGE MEASUREMENT

This is aimed at measuring the TIV of the experimental DC CB. Special focus in this case will be on the rate-of-rise of the TIV, the residual voltage at current zero, the peak value and the duration of the TIV.
Referring to Figure 2-1, voltage is measured at three different locations

- Voltage across vacuum interrupter
- Voltage across MOSA branch
- Voltage across the entire test object

Standard resistor- capacitor (RC) voltage dividers are used for this purpose. For example, NorthStar VD150 (with maximum measuring frequency of 20 Mhz), Heafely 150 kV and 1600 kV are the voltage dividers used.
Later when multiple vacuum interrupter modules are applied, the voltage sharing among the modules will be investigated. Thus, there will be a need to measure voltage on floating potential or rely on the difference between measurements.

2.2.3 TEMPERATURE MEASUREMENT

The MOSA branch will absorb and dissipate considerable amount of energy during tests. As a result, there will be a temperature rise in the MOSA columns. The main purpose is to study temperature rise of MO-varistor columns as a result of a specified energy injection and to determine the cooling down characteristics of the columns.

As discussed in Section 2.2, the MOSA columns are designed in such a way that access to temperature measurement at the middle of the column is provided. This is a location within a column at which the least heat dissipation to the environment is occurring. However, this position is not at ground potential. This means, temperature is measured at high potential. Hence, temperature measurement systems such as thermocouples and thermistors cannot be used for this purpose. Rather, fibre optic (FO) based temperature measurement solution is used in this case, see Figure 2-33. A multi-channel FO based temperature measurement system with data acquisition rate as high as 10 Hz per channel is used. This system is Qualitrol, Neoptix OmniFlex-2 temperature measurement system shown in Figure 2-34. The FO temperature probes shown in Figure 2-33 has temperature measurement range from -50 ºC to 250 ºC with system accuracy of ±1 ºC.

Moreover, the surge arrester modules are designed so that all the columns are visible to a single thermal (infrared) camera from one direction. Thus, a thermal image showing an overview of the temperature of all the columns can be taken. This is used to monitor and assist the actual temperature and current measurements.

This project has received funding from the European Union's Horizon 2020 research and innovation programme under grant agreement No 691714.

Figure 2-33: Fibre optic temperature probe – Qaulitorl T2S probe

Figure 2-34: Fibre optic based temperature measurement system. Signal conditioner and data acquisition Qaulitrol, Neoptix, OminiFlex -2 system

This project has received funding from the European Union's Horizon 2020 research and innovation programme under grant agreement No 691714.

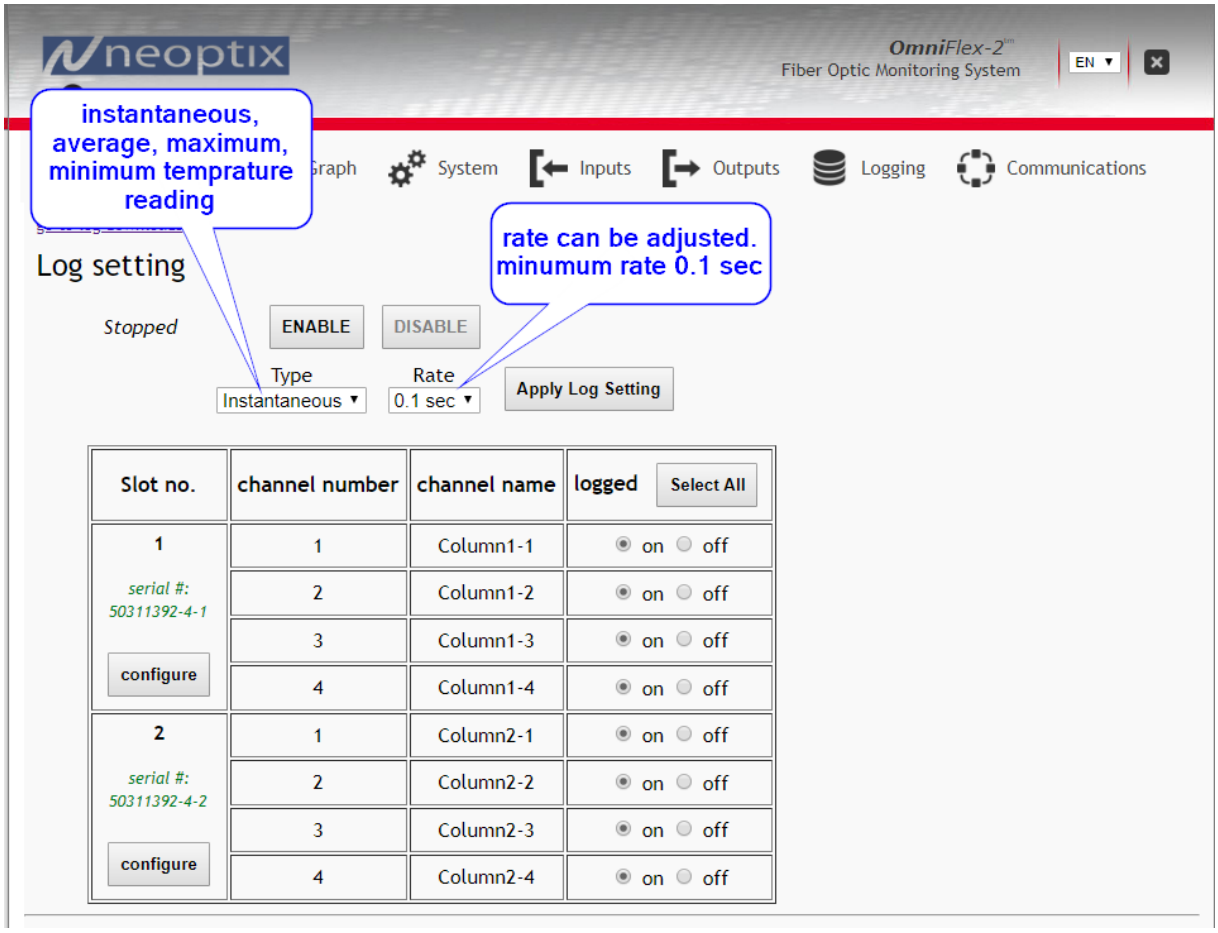

Figure 2-35: Temperature data acquisition settings

The measurement system has 8 channel temperature data acquisition system, each of which has data scanning rate of as low as 10 samples per second .

The temperature data can be stored for later analysis and processing. Thus, current sharing measurement is cross validated by temperature measurement since the temperature rise of each column is proportional to the current flowing through the column.

2.4 SPECIFICATION OF THE CURRENT INJECTION CIRCUIT

The current injection circuit consists of pre-charged injection capacitor (C_P), injection reactor (L_P) and triggered spark gap.

2.4.1 INJECTION FREQUENCY, CHARGING VOLTAGE AND PEAK CURRENT OF INJECTED CURRENT

In order to investigate current interruption performance of vacuum interrupter under various current injection conditions, different values of injection capacitor and injection reactor are used. The capacitor bank used for this

This project has received funding from the European Union's Horizon 2020 research and innovation programme under grant agreement No 691714.

purpose is shown in Figure 2-36. The values of the capacitors, the injection reactors and the resulting injection frequency considered in the investigation is shown in Table 7. The injection current with peak value of 20 kA is assumed as it creates sufficient number of current zeros when interrupting current up to 16 kA.

The capacitor and inductor values in Table 7 are obtained using the following mathematical expressions.

$$C = \frac{I_P}{V_C} * \frac{1}{2\pi f}$$

And

$$L = \frac{V_C}{I_P} * \frac{1}{2\pi f}$$

Where I_P is the peak value of the injection current, V_C is the pre-charge value of the injection capacitor and f is the frequency of the injection circuit.

Table 7: Injection circuit parameters and the resulting rate of change of current near current zero when interrupting various current magnitudes. The pre-charge voltage of the capacitor is 26 kV

Frequency (kHz)	1	2	3	4	5	6	7	8	9	10
Capacitor (µF)	127.3	63.7	42.4	31.8	25.5	21.2	18.2	15.9	14.1	12.7
Inductor (µH)	199	100	66.3	49.7	39.8	33.2	28.4	24.5	22.1	20
di/dt @2 kA (A/µs)	125	250	375	500	625.2	750.2	875.2	1000.3	1125.3	1250.3
di/dt @10 kA (A/µs)	108.8	217.7	326.5	435.3	544.1	653.0	761.8	870.6	979.5	1088.3
di/dt @16 kA (A/µs)	75.4	150.8	226.2	301.6	377	452.4	527.8	603.2	678.6	754

For the purpose of creating current zero in the vacuum interrupter, the pre-charge voltage can be chosen as long as current zero is created for the rated interruption current. That means it depends on the inductance of the loop (could be with additional inductance) between the charged capacitor and the vacuum interrupter. The capacitor together with this inductance influences the di/dt at current zero through the injection frequency. However, the capacitor should be able to be charged to and withstand the peak value of TIV. It is imperative to think that in the field this capacitor is charged from the system and hence the charging voltage of the capacitor is usually the same as the rated system voltage. For a single interrupter case, the charging voltage of the experimental DC CB is set to 26 kV.

For high-speed making of the injection circuit, the plasma triggered spark gap is used. This can be seen in Figure 2-37.

This project has received funding from the European Union's Horizon 2020 research and innovation programme under grant agreement No 691714.

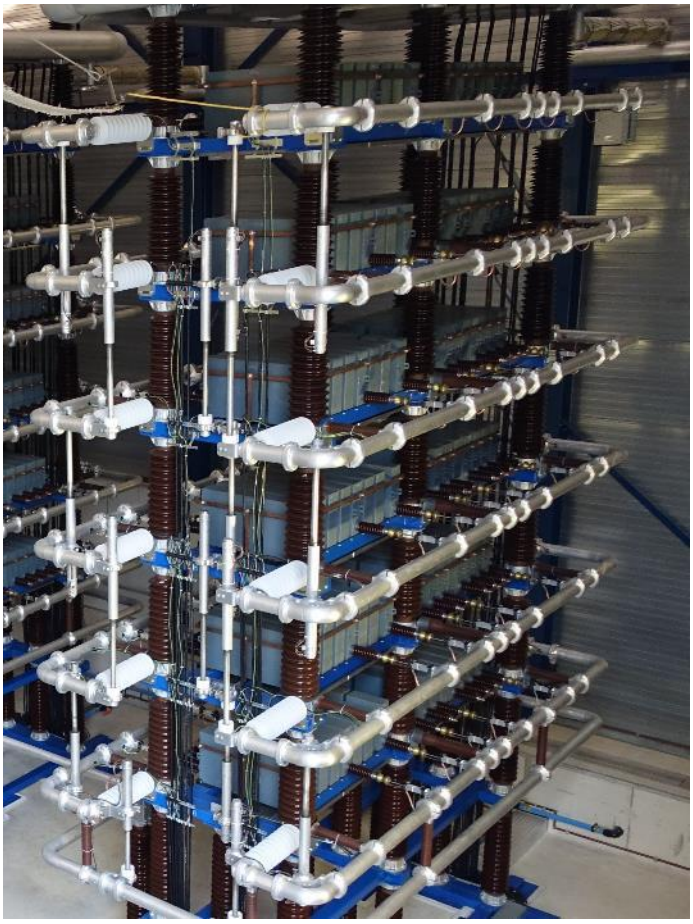

Figure 2-36: Mobile Capacitor Bank for counter current injection circuit

Figure 2-37: Triggered spark gap used as making switch

This project has received funding from the European Union's Horizon 2020 research and innovation programme under grant agreement No 691714.

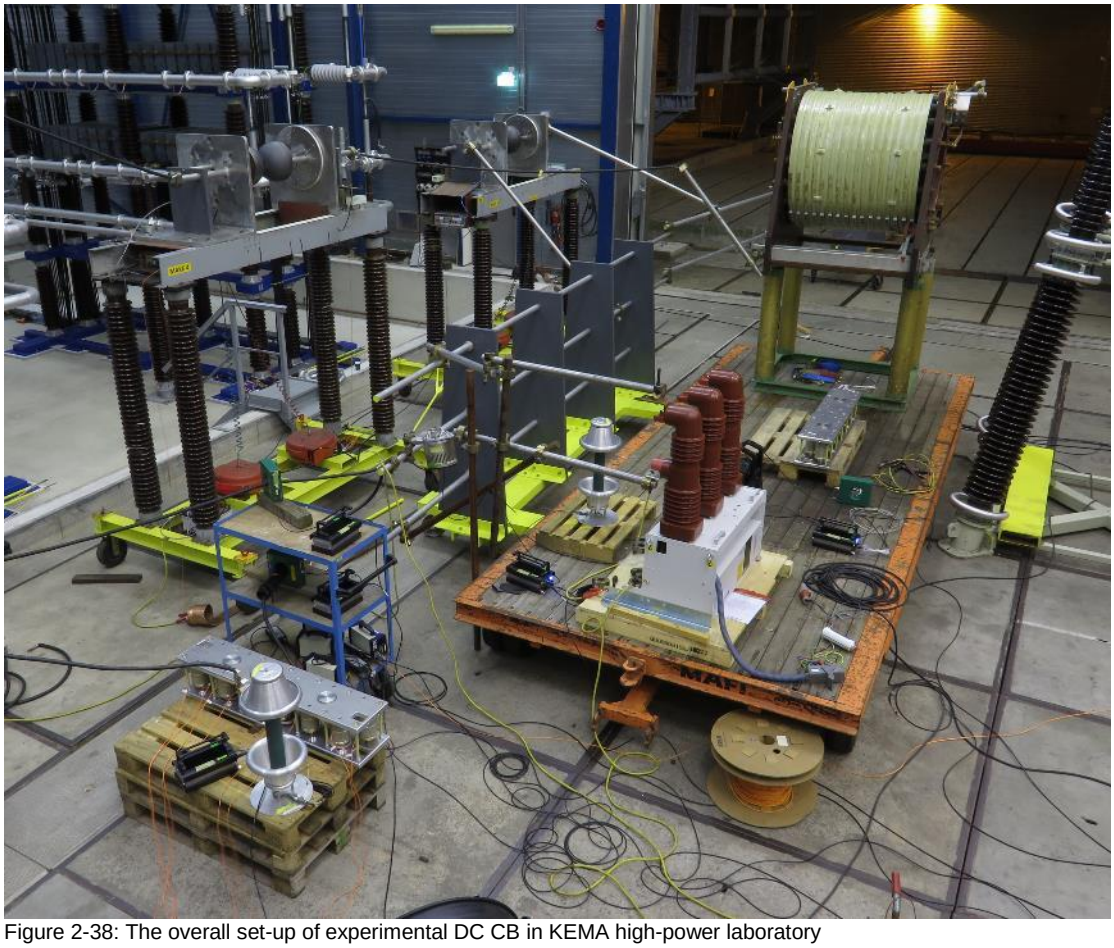

Figure 2-38: The overall set-up of experimental DC CB in KEMA high-power laboratory

2.6 SPECIFICATION AND DESIGN OF THE MAIN POWER AC CIRCUIT

The main circuit supplying the current, voltage and energy stresses is discussed in detail in D5.6, D5.7 and D10.1. To focus only on the current interruption performance of vacuum interrupter, the test circuit with power frequency of 30 Hz is chosen. This results in a lower peak value of prospective current as well as shorter current loop duration. This reduces the wear on the vacuum interrupter contacts in case the experimental DC CB fails to clear the current. Later when the circuit components are chosen for optimal performance, test circuit supplied by power source running at 16.7 Hz is used. In the latter case the focus is within the energy handling capability of the MOSA.

2.7 MULTI-UNIT HVDC CIRCUIT BREAKER

HVDC circuit breakers are designed for high-voltage (HV) or extra high-voltage (EHV) systems by cascading two or more HVDC circuit breaker units or modules. Depending on the design and technology of HVDC circuit breaker, these modules could share one or more components.

This project has received funding from the European Union's Horizon 2020 research and innovation programme under grant agreement No 691714.

When cascading number of HVDC circuit breaker modules, different configurations can be realized. The impact of MOSA connection to the VIs will be investigated (i.e. MOSA connection per module vs MOSA connection across a series connection Vis as shown in Figure 2-40).

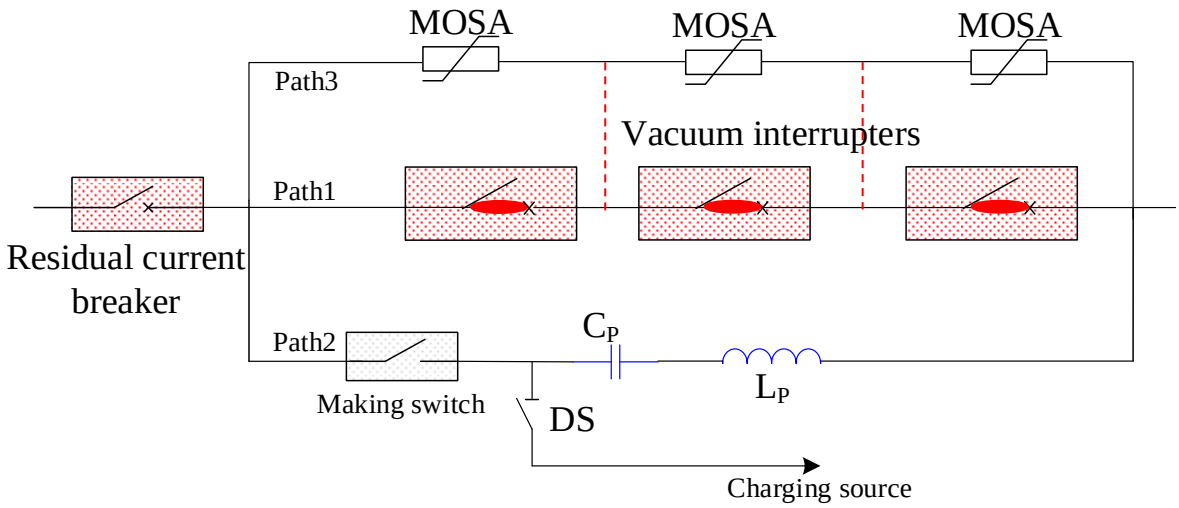

Figure 2-39: Schematic of multi-module experimental HVDC circuit breaker

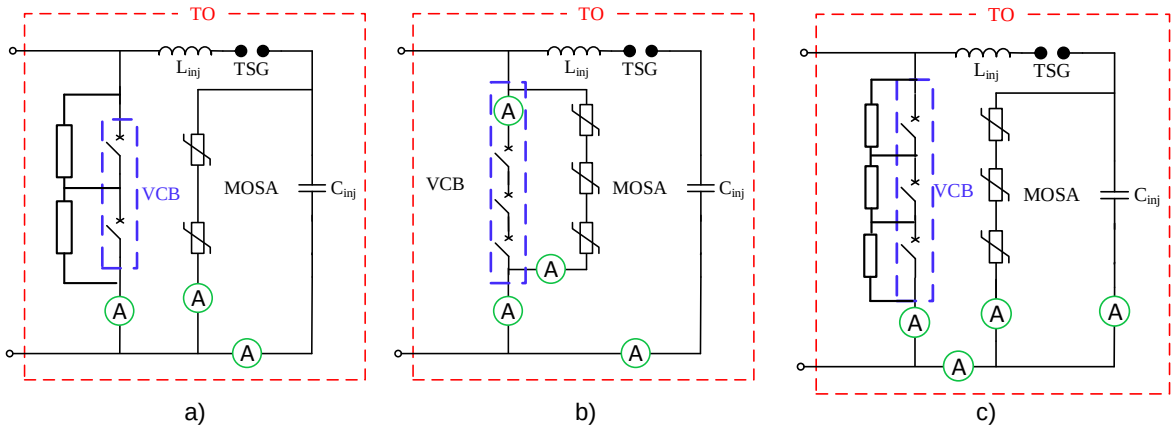

Figure 2-40: Possible configuration of double and triple break experimental DC CB

This project has received funding from the European Union's Horizon 2020 research and innovation programme under grant agreement No 691714.

Figure 2-41: Photo of 9 MOSA stacks for a multi-break experimental DC circuit breaker

2.7.1. VOLTAGE GRADING ELEMENTS

One of the main issues of cascading HVDC circuit breaker modules is equal sharing of voltage stress among the modules. External voltage grading elements such as grading capacitors are used to ensure proper voltage distribution among the modules. Figure 2-42 shows grading capacitors with values in the range of 700 pF – 25000 pF.

Figure 2-42: Grading capacitors that can be used for a multi-break experimental HVDC circuit breaker

This project has received funding from the European Union's Horizon 2020 research and innovation programme under grant agreement No 691714.

3 DESCRIPTION OF PURPOSE OF THE SET-UP

The main goal is to quantify electrical and thermal stresses on the components/sub-components of HVDC circuit breakers. To quantify these stresses access to measurements of the electrical parameters across/through the sub-components of HVDC CBs is necessary. Therefore, in this task it is preferred to set-up an experimental HVDC CB (independent of any of the manufacturers) for this investigation. Here, it must be clear that the aim is not to study the overall performance of the experimental HVDC CB. The stresses on the common components of most HVDC CBs such as vacuum interrupters and metal oxide surge arresters (MOSA) are of interest in this task. The main stresses that are investigated using the experimental HVDC CB are described below.

3.1 VOLTAGE STRESS

In normal operation, when the HVDC circuit breaker/any of its internal components does not see voltage stress. However, one of the unique feature if the HVDC CB is the generation of transient interruption voltage (TIV) during current interruption. This voltage must be higher than the system voltage in which the HVDC CB is to be installed. Thus, there is a self-imposed voltage stress by the HVDC circuit breaker. In addition, there is a system voltage applied across the HVDC circuit breaker after current interruption. This must be considered during testing of HVDC circuit breakers since it ensures whether there is any late (dielectric) breakdown of the components of the breaker under test. Two important aspects of voltage stress come into view as discussed below.

3.1.1 MAGNITUDE OF TIV

This is related to the peak value of the TIV during the current interruption process. In general, the value of the TIV peak is determined by the design of the MOSA branch of the HVDC CB. During the transient period, the TIV has different values at different time stages. The highest peak appears during the first transients because of oscillations caused by the interaction of the stray inductance with capacitors within the breaker. The magnitude and frequency of this oscillation depend on the design (compactness) of the whole breaker set-up. These oscillations decay soon and steady state TIV is reached. The value and the duration of the steady state TIV is determined by the current being interrupted, the (actual) system voltage and the energy in the circuit. However, the transient during the first period has significant impact on the success of the current interruption as the other components such the main interrupter sees this voltage. This will be investigated with detailed measurements in this task.

3.1.2 MAGNITUDE OF INJECTION CAPACITOR RESIDUAL VOLTAGE

In all cases, there is residual voltage as a result of the remaining charge across the counter current injection capacitor of the HVDC CB. This becomes conspicuous when interrupting low currents. The impact of the residual voltage on the internal components of the HVDC circuit breaker will also be studied.

This project has received funding from the European Union's Horizon 2020 research and innovation programme under grant agreement No 691714.

3.1.3 RATE-OF-RISE OF TIV

Besides the peak value, the rate-of-rise of the TIV is another crucial stress on the components of the HVDC circuit breaker. For example, the contacts of the mechanical interrupter which has just been arcing/opening must deal with the rising TIV. This has an impact on the necessary minimum arcing duration as well as the gap length of the main interrupter. The rate-of-rise the TIV depends on the value of the interrupted current as well as the size and (residual) charge of the current injection capacitor, as well as on stray elements. The lower the interrupted current the lower the rate of rise of the TIV; however, the larger the magnitude of the initial TIV voltage due to the remaining charge across the capacitor. Thus, for a lower current, it is the initial TIV which influences the performance of the vacuum interrupter. Also, the di/dt at current zero is higher while interrupting lower current and thus the rate of thermal recovery has significant impact.

3.2 CURRENT STRESS

The HVDC circuit breaker must not only be designed to interrupt the maximum current, but also low currents such as load current.

3.2.1 CURRENT MAGNITUDE

The magnitude of the interruption current determines the thermal energy in the vacuum arc. The likelihood of the current interruption at next current zero depends on the thermal energy in the arc plasma until the current zero.

3.2.2 RATE OF CHANGE OF CURRENT (DI/DT)

There are two aspects of the rate of change of current. The first is the rate of change of the system fault current and the rate of change of current through the vacuum interrupter at current zero. Both have impact on the interruption performance. For example, the rate of change of system current determines the number of current zeros that can be created with a given injection current. Due to parasitic resistance (damping) the injection current decays. Coupled with this damping, if the system current is rising at higher di/dt, the number of current zeros that can be created are reduced.

On the other hand, the rate of change of current through the vacuum interrupter during current interruption process depends on the magnitude of current being interrupted as well as the frequency of the injection current and on charging voltage of the injection capacitor. Given, the injection frequency and the peak value of the injection current, the lower the interruption current, the higher the di/dt at current zero or vice versa.

3.3 ENERGY STRESSES

The other unique feature of the HVDC circuit breaker is the energy absorption. While dealing with the stresses mentioned above the HVDC circuit breaker absorbs the magnetic energy in the system. This energy is dissipated in the MOSA branch in the form of thermal energy. The maximum energy that the MOSA columns or a given varistor block can absorb is limited for a safe operation. If more energy than these components can handle is

This project has received funding from the European Union's Horizon 2020 research and innovation programme under grant agreement No 691714.

imposed, it will lead to damage/failure. There are different forms of failure such as puncture, thermal run away and/or cracking. Each of the mentioned failure modes have different causes. This will be investigated with experiments in the lab.

It must be noted that while the energy absorbing branch is stressed with energy, the other components such as the vacuum interrupter in the mechanical DC CB or the ultra-fast disconnector (UFD) and the IBGTs in the main breaker branch in hybrid DC CB are stressed by the voltage produced by the MOSA.

This project has received funding from the European Union's Horizon 2020 research and innovation programme under grant agreement No 691714.

4 EXAMPLE CASE TEST RESULT ANALYSING COMPONENT STRESSES

In this chapter a test result showing the internal measurements of the experimental DC CB is described. The purpose of this is to show the working of the set-up. The detailed analysis of large number of test results under various test parameters is performed in D10.3 which follows this document.

Figure 4-1 shows typical test result of experimental DC CB. The experimental DC CB is operated in such a way that the contacts of the vacuum interrupter (VI) are separated at T_1 in Figure 4-1. Once the contacts of the VI are separated, current continue to flow through an arc, established between the parting contacts. The VI contacts are let to arc for a while until it reaches sufficient gap length to withstand subsequent transient interruption voltage (TIV). This shown as the arcing (between double arrow) on Figure 4-1 top graph. The gap length and hence arcing duration is one of the parameters of investigation of the experimental DC CB. In other words, what is the minimum gap length sufficient for successful DC current interruption will be investigated.

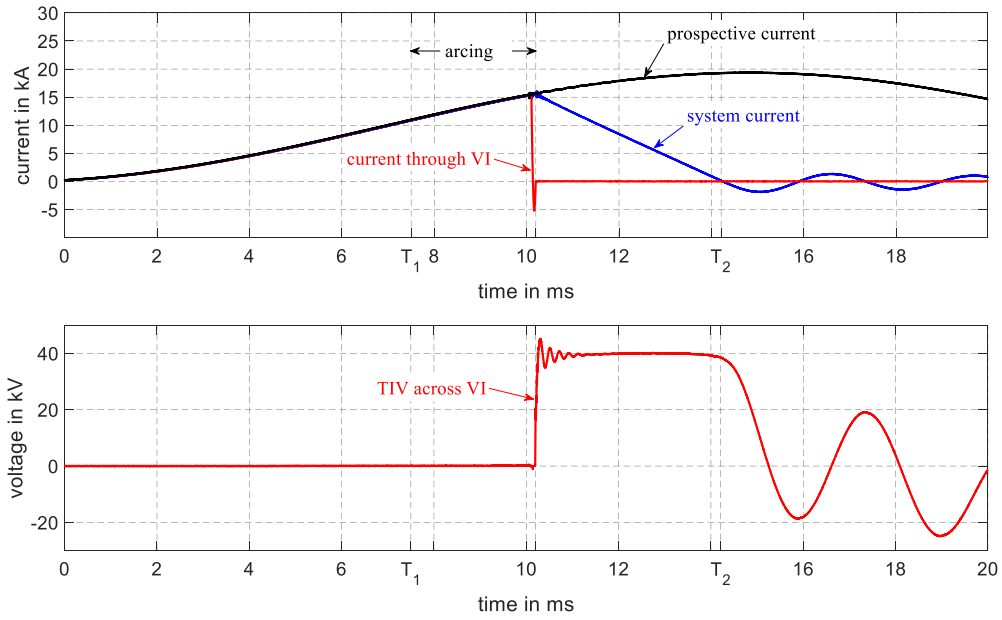

Figure 4-1: Example case test result of experimental DC CB

After sufficient gap length is reached by the moving contact(s) of the VI, a counter current is injected from a pre-charged capacitor to create a local current zero through the arcing VI. This is shown by the red trace on Figure 4-1 top graph. It can be seen that current zero is created at VI contacts and the arc is extinguished as a result where current is no longer flowing through VI. Thus, the system current is commutated from the VI to the injection circuit path (path 2, in Figure 2-1). The commutation of current into capacitor results in charging of the capacitor until the voltage is limited by the MOSA connected in parallel with the capacitor (see path 3 in Figure 2-1). This is shown by the TIV trace in Figure 4-1 bottom graph. The TIV is higher than the source voltage producing the short-

This project has received funding from the European Union's Horizon 2020 research and innovation programme under grant agreement No 691714.

circuit current. Therefore, after the TIV is generated the system current is suppressed to zero or to a small oscillating current (see after T_2) that can be cleared by residual current breaker. In Figure 4-1 top graph, prospective current is added to show what would happen in case the circuit breaker failed to clear.

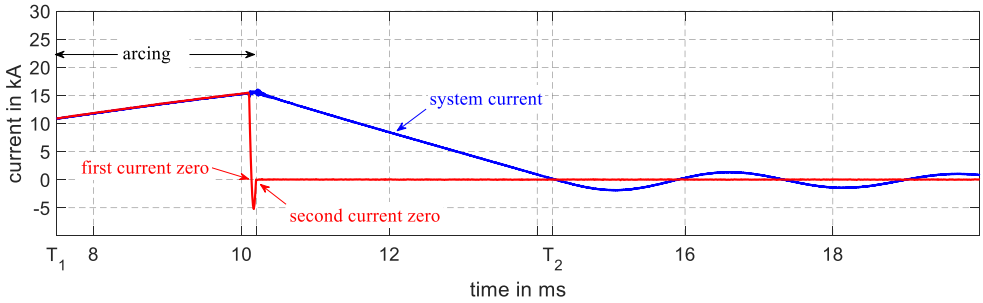

Figure 4-2: closer look at current through the VI during counter current injection

Figure 4-2 shows the zoomed version of current though the VI during counter current injection. It can be seen that the VI does not clear current at first opportunity (first zero), rather at the second zero in this case. There are a lot of factors determining the success rate of current interruption at first current zero which include, the peak value of the interruption current, the rate of change of current at current zero, vacuum interrupter contact design, the gap length, etc. The impact of these parameters will be investigated in D10.3.

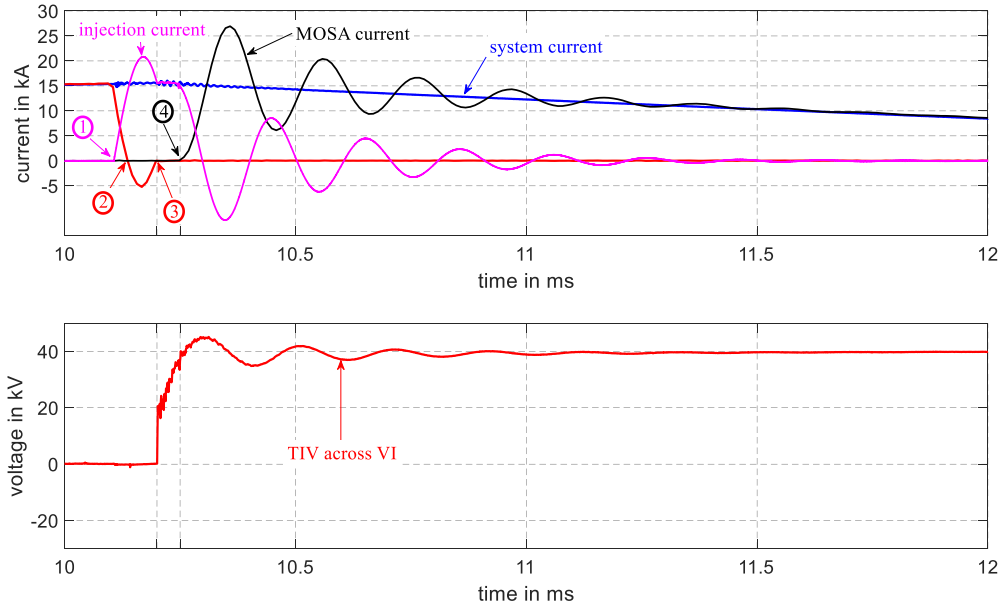

Figure 4-3: Internal current measurements of experimental DC CB

Figure 4-3 depicts the sequence of events during current interruption by showing current measurements through several branches. In relation to Figure 4-3, the sequence of events following the opening of VI contacts are as follows. At point (1) (see the magenta trace), the plasma triggered spark gap is fired, resulting in counter current injected from the pre-changed capacitor. As a result of counter current, the current through the VI contacts reduces (see the red trace) at the same rate at which the counter current is increases. At point (2) the VI fails to clear at first zero and the counter current continue to rise to its peak value of about 20 kA. The counter current is a high

This project has received funding from the European Union's Horizon 2020 research and innovation programme under grant agreement No 691714.

frequency (4 kHz) current and must have higher peak than the interruption current. Next, as the injected current decreases from its peak value, it creates another current zero through the VI contacts. This time the VI succeeds to clear the current flowing through its contacts, see point (3) in Figure 4-3. As mentioned earlier, the system current flows into the capacitor and hence, charging it. This can be seen from magenta trace on Figure 4-3 between points (3) and (4) where the current through the injection circuit is the same as the system current. At current zero (point (3), significant amount of charge remains across the capacitor. This is a reason why the TIV at once jumps from almost zero to about 20 kV. This is one of the challenges to the VI as is results in extreme rate of rise of voltage (du/dt). From this point on the TIV rises from 20 kV to about up to 35 kV at which point the current starts to commutate to MOSA. At point (4) on Figure 4-3 the MOSA starts to conduct until the system current is suppressed. The oscillation observed on the MOSA current and injection current is due to the interaction of stray inductance because of connection from the MOSA to the injection branch. The more compact the set-up is the less this oscillation is. Of course, this oscillation decay very quickly. Once the system current is commutated to the MOSA, the TIV value follows the current magnitude flowing though MOSA as discussed in Section 2.2.

This project has received funding from the European Union's Horizon 2020 research and innovation programme under grant agreement No 691714.

5 SUMMARY

This document presented the major components of the experimental DC CB set-up for investigation of sub-component stresses in a laboratory environment. Most of the components used in the set-up are readily available standard laboratory equipment. The document provides the specification of the components used to setup active current injection DC CB. The major components of focus are the vacuum circuit breaker, the metal oxide surge arrester (MOSA), the injection capacitor and inductor.

A special attention has been given to the design of MOSA which constitutes a crucial part of all technologies of HVDC CB. The differences in use of MOSA for HVDC circuit breaker and for over-voltage protection in power systems is highlighted in this deliverable. In addition, the impacts of the varistor block dimension on the I-V characteristics is discussed in detail by supporting with experimental verifications. The design consideration and procedure of MOSA for HVDC CB application is illustrated with the actual specification of the experimental DC CB as an example case. Moreover, a crucial step in the construction of the MOSA for HVDC CB, the column matching procedure, is described using the actual laboratory measurements and procedures. In order to cope with high-energy absorption requirement, the HVDC CB constitute MOSA stack consisting of several columns. The impacts of the number of columns on the TIV of the HVDC CB is demonstrated with real measurements.

The document also provides the details of instrumentation needed for investigation of subcomponent stresses. Special multi-channel current measurement with a possibility to perform current measurement on high-potential are presented. In addition, various voltage measurement, multi-channel optical based temperature measurement system for real-time monitoring of MOSA temperature is used.

This deliverable highlights the important electrical parameters of HVDC CB to studied in D10.3. Finally, it presents an example case test result recorded during current interruption by experimental DC CB set-up in the laboratory.

This project has received funding from the European Union's Horizon 2020 research and innovation programme under grant agreement No 691714.

BIBLIOGRAPHY

[1] T. Heinz, V. Hinrichsen, L.-R. Jänicke, E. D. Taylor and J. Teichmann, “Direct current interruption with commercially available vacuum interrupters,” in *XXVI Int. Symp. on Discharges and Electrical Insulation in Vacuum*, Mumbai, 2014.

[2] L. LILJESTRAND, M. BACKMAN, L. JONSSON, M. RIVA and E. DULLNI, “DC VACUUM CIRCUIT BREAKER,” in *24th International Conference on Electricity Distribution*, Glasgow, 2017.

[3] J. Woodworth, “Helping Understand the VI Characteristic Curve,” INMR, 13 01 2018. [Online]. Available: http://www.inmr.com/helping-understand-characteristic-curve/#!prettyPhoto. [Accessed 15 11 2018].

[4] V. Hinrichsen, Metal-Oxide Surge Arresters in High-Voltage Power Systems, Berlin and Darmstadt: Siemens, 2011.

[5] ABB Switzerland Ltd., *Overvoltage Protection Metal Oxide Surge Arresters in Medium Voltage Systems,* ABB, 2011.

[6] N. A. Belda and R. P. P. Smeets, “Test Circuits for HVDC Circuit Breakers,” *IEEE Transactions on Power Delivery,* vol. 32, no. 1, pp. 285-293, 2017.

[7] N. A. Belda, C. Plet and R. P. P. Smeets, “Analysis of Faults in Multi Terminal HVDC Grid for Definition of Test Requirements of HVDC Circuit Breakers,” *IEEE Transactions on Power Delivery,* vol. 33, no. 1, pp. 403-411, 2018.

[8] PROMOTioN Deliverable 5.3, “Fault Stress Analysis of HVDC Circuit Breakers,” 2016.

[9] PROMOTioN Deliverable 5.6, “Software and analysis report on candidate test-circuits and their effectiveness,” PROMOTioN Project, 2017.

This project has received funding from the European Union’s Horizon 2020 research and innovation programme under grant agreement No 691714.